ATTACHMENT 10

Appendix A

Definition of a Source Water Volume for the South Bay Power Plant San Diego, California.

Definition of a Source Volume for the South Bay Power Plant San Diego Bay, California

by

David A. Jay
Associate Professor
Department of Environmental and Biomolecular Systems
Oregon Health & Science University
Beaverton, OR

John L. Largier
Associate Research Oceanographer
Scripps Institution of Oceanography
University of California, San Diego
La Jolla, CA

Prepared for Tenera Environmental and Duke Energy, North America

19 December 2003

1.0 INTRODUCTION

The purpose of this report is to provide an oceanographic basis for definition of a source volume for entrainment calculations applicable to the South Bay Power Plant (SBPP), which withdraws water from San Diego Bay, California. This report defines the broader context of the power plant (**Section 2**), summarizes estuarine circulation processes relevant to larval entrainment (**Section 3**), quantifies tides, tidal currents, and tidal dispersion, (**Section 4**) and defines the source volume (**Section 5**). **Section 4** uses tidal elevation and current meter data to: a) determine the part of the source volume above Mean Lower Low Water (MLLW), and b) define patterns of tidal heights, tidal currents, and tidal dispersion, all decisive factors in defining the boundaries of the source volume. The discussion and analyses of **Sections 3** and **4** justify the definition of a south bay source volume in **Section 5** and confirm in a quantitative manner earlier definitions of eco-regions in San Diego Bay (e.g., Merkel and Associates 2000). In effect, the Coronado Narrows may be considered to be the "mouth" of south bay. The Narrows is, therefore, a logical seaward boundary for the SBPP source volume.

2.0 SAN DIEGO – BROADER CONTEXT

2.1 Physical Setting

San Diego Bay is a crescent-shaped embayment on the southern California coast, extending from 32º 36' N to almost 32º 44' N (**Figure 1a**). It is separated from the sea by a sand spit extending north and west from Imperial Beach almost to Point Loma, which limits the westward extent of the bay. Shore protection has stabilized the formerly shifting sands of the peninsula; these are now known as Shelter, Harbor, and North Islands. The present axial length of the bay is about 24.5 km, from the tip of Pt Loma to the mouth of the Otay River, south of SBPP. Due to the curvature of San Diego Bay, the mouth has a north-south orientation, and a vessel entering the bay from the ocean travels almost due north. However, the channel curves sharply east about 2 nautical miles (NM) north of the entrance, such that the portion of north San Diego Bay west of downtown San Diego is oriented east to west, with east being the landward direction. Moving further in the landward direction, the bay then trends southeast and then south-southeast, such that south bay, near the SBPP trends almost north-south, with south being the landward direction.

The bay has two basic geomorphic portions, an outer bay (including the entrance and north San Diego Bay) seaward of Coronado Narrows (13.5 km from the entrance) and an inner bay landward of the Narrows, known as south bay. The mouth of the bay is stabilized and constricted by Pt Loma to the west and Zuniga Jetty to the east, enclosing a navigation channel with a controlling depth of about 45 ft on MLLW. This dredged channel extends into north San Diego Bay, most of the way to the Narrows. The outer half of the bay is relatively narrow (1-2 km) and deep, 25-45 ft in most places. Adjacent harbor facilities make the shoreline of north bay quite complex, and most protected peripheral areas are relatively shallow, <20 ft. Coronado Narrows, the landward limit of the outer bay, is 40-45 ft deep and only 600 m wide. The more landward south bay forms a broad (2-4 km), predominantly shallow embayment, while remaining mostly subtidal. Only a channel along the eastern shore of south bay is fairly deep.

Just landward of the Narrows, the channel is 30-40 ft deep and ~1 km wide. It narrows and shallows toward the south, being 200 m wide and 20-25 ft deep near Sweetwater Channel. At the entrance to Chula Vista Harbor, it is only approximately 100 m wide. It shallows to 10 ft as it approaches the SBPP. While south bay has some intertidal flats, most shorelines are protected, and extensive salt ponds have been removed from the estuary south of the SBPP, along the Otay River. The SBPP is located in south bay, and south bay forms the source volume for SBPP entrainment calculations.

2.2 Climate and Oceanographic Context

San Diego Bay opens to the coastal waters of the southern part of the Southern California Bight, about 10 km north of the California-Mexico border. The Southern California Bight is characterized by the absence of strong northerly upwelling winds, in contrast to central and northern California (north of Pt Conception) and in contrast to the coast of Baja California (particularly south of Ensenada). The southward airflow separates from the coast at Pt Conception and connects again with the coast south of the border. The core of the large-scale California Current does likewise, flowing southward on the west side of the Channel Islands. In the southern Bight, near San Diego, there is typically a northward counter current of California Current waters. Close inshore, however, there appears to be a tendency for southward currents (Engineering Science 1988) past Pt Loma.

San Diego Bay exchanges waters primarily with the embayment made by Pt Loma and Punta Bandera (just south of Tijuana) to the Coronado Bight. During winter, these waters are cool (12-15^{o} C) and weakly stratified (unpublished data, Largier et al.). During spring-summer-fall, however, these waters are strongly stratified with a shallow thermocline and vertical temperature differences on the order of 10^{o} C. Surface waters warm to a maximum of between 20^{o} C and 24^{o} C. Cooler surface water is frequently observed outside the mouth of San Diego Bay, indicating localized upwelling associated with Pt Loma and the mouth of the bay (**Figure 1b**). This may be due to the southward flow past Pt Loma, local wind forcing, coastal trapped waves generated by strong winds off central Baja California (Pringle and Riser 2003), and/or the action of tidal flow to/from the bay. This cold nutrient-rich water can be observed moving into San Diego Bay.

San Diego Bay is characterized by a semi-arid climate, with an average rainfall of only ~0.25 m. Most rainfall occurs during the November to March period, with summer rainfall being negligible in many years (Largier 1995). The amount of precipitation is considerably less than the estimated annual evaporation, typically ~1.6 m. Most of the evaporation occurs in summer and the early fall, resulting in markedly hypersaline conditions from late summer until the occurrence of winter rains. While typical winds in the area are moderate (<5 ms^{-1}), there is a strong diurnal cycle, with a sea-breeze bringing cool air onshore many afternoons. Strong, hot easterly winds may occur during Santa Ana conditions; these occur most frequently during fall, and may bring fire weather, notably the case in 2003. The coldest conditions occur during clear winter weather. Occasional winter storms may also bring strong onshore winds. While the bay is relatively protected from ocean swell, local winds may raise wind waves of up to 2 ft. The marked seasonality of weather conditions, leading to freshwater input in winter and hypersalinity in summer, is an important factor in evaluating oceanographic observations. Most

oceanographic time series for the system as a whole are of only a few months duration, reflecting patterns typical of a particular season rather than average conditions.

2.3 Geomorphic Setting

San Diego Bay has been shaped by tectonic forces, sea-level rise and fall, and human alterations, as described by IRC (1980). Pt Loma and possibly North Island are fault blocks that strongly constrained the form of the bay. During the last ice, the San Diego, Sweetwater, and Otay rivers deepened their channels through the bay (**Figure 2**). As sea level rose and then stabilized after the last ice age ca. 7,000 YBP (years before present), West-Coast estuaries, probably including San Diego Bay, began to assume their modern forms. The spit that separates the bay from the ocean formed in the lee of Pt Loma, under the influence of tidal currents and the coastal wave regime. Before its permanent diversion to Mission Bay in 1852, the San Diego River alternately emptied into San Diego and Mission bays, carrying with it considerable quantities of poorly sorted sediment, with sizes ranging from clay to gravel. The location of the mouth of the San Diego River was unstable, and the sediment load to San Diego Bay was deemed a hindrance to navigation, resulting in the 1852 diversion. In comparison to the San Diego River, the Otay and Sweetwater rivers were evidently lesser, though not insignificant, sources of sediment.

Loss of sediment supply, dredging, and filling of shoreline areas has greatly altered the form and sedimentology of San Diego Bay—compare **Figure 1a** to the 1857 configuration (**Figure 3**). Surficial sediments are mostly sands near the bay mouth and along the bay side of the spit (IRC 1980). Sediments become finer toward the head of the bay and along its east side, with muds (clay and silt) predominating in some areas. Modern San Diego Bay sediments are typically 1.5 to 6m deep, in areas where they have not been removed altogether by dredging. These sediments rest upon 12–18 m of unconsolidated sand and silty sand (likely post ice-age), which in turn rest upon ancient, more consolidated sediments. Dredging of much of the bay has removed the finer over-burden, exposing relict sands in many areas. However, the natural channel in 1857 was in much the same location as the modern channel.

2.4 Ecological regions

The San Diego Bay system possesses very significant habitat value, having for example, the largest area of eelgrass beds (505 ha) of any system in the Southern California Bight (Merkel and Associates 2000). In an analysis of controls on eelgrass occurrence, Merkel and Associates divided San Diego Bay into four ecological regions (**Figure 4**). The North Eco-region includes most of the deep navigation channel and the generally deep area landward to the Navy wharf. The North-Central Eco-Region covers the predominantly deep area from the Navy Wharf through the Coronado Narrows to the Coronado Bridge. Landward of this point is the South-Central Eco-region, which is transitional between the deeper areas seaward of the Coronado Narrows and south bay. The SBPP is contained within the South-Bay Eco-Region, which is predominantly shallow subtidal and intertidal; this eco-region contains most of the bays' eelgrass beds. The salt pans south of SBPP are not part of the estuary proper (or any of the above eco-regions) but nonetheless contain significant bird habitat. Our division of the bay into an outer portion and south bay is very similar to the system adopted by Merkel and Associates, with a

minor shift in boundaries between the inner and outer bays. Merkel and Associates used the Coronado Bridge as a convenient boundary between the two inner and two outer eco-regions. We have used instead a boundary that is at the narrowest point of the bay (at least landward of Ballast Pt.); this boundary is about 1.5 km seaward of Merkel and Associates' boundary. This difference in boundaries has no real ecological significance. Our boundary is, however, defendable in terms of the structure and hydrodynamics of the bay, and makes optimal uses of available oceanographic information.

2.5 Tides and Currents

Tides have been measured over the last 20 years at a variety of locations in San Diego Bay providing a good basis for understanding tidal processes. Tides in San Diego Bay are mixed diurnal-semidiurnal, with the semidiurnal (twice-daily) component being stronger than the diurnal (once-daily) component. The ratio of semidiurnal to diurnal forcing varies from 1.29 near the ocean entrance (Ballast Pt., TG5) to 1.41 in south bay (station SB); it is 1.36 at the reference station (TG0). Currents are relatively weak throughout San Diego Bay, especially south of the Narrows. This is a natural consequence of the closed nature of the head (southern end) of south bay. Thus, the behavior of the tides in San Diego Bay is typical of systems with relatively weak friction and a modest convergence in channel cross-section toward the head of the bay. Because the head of south bay is closed, along-channel currents nearly vanish there, leading to what is called a "standing-wave" tide. In this situation, tidal currents are absent at low and high water, while the bay fills and empties most rapidly at mid-tide, the time of the most rapid changes in surface elevation. High water and low water are nearly simultaneous throughout the bay, and peak currents at most locations lead high water by almost quarter of a tidal cycle, or 70 to 90º, though there are some localized variations in this feature. The standing-wave character of the tide also leads to a modest resonance or amplification of the tide in San Diego Bay and perhaps the bight south of Pt Loma. Thus, the diurnal tidal range (distance Mean Higher High Water [MHHW] and MLLW surfaces) at Ballast Pt. (TG5) is 1.67 m, slightly larger than the range at La Jolla (1.62 m) in the adjacent coastal ocean. The range increases to 1.75 m San Diego (TG0), and to 1.80 m at station SB near the SBPP.

The tidal prism, the volume of tidal flow that goes in and out of San Diego Bay every day, is an indicator of the importance of tidal processes to the bay. For a bay that is short relative to the tidal wavelength, it is usual to approximate the average tidal prism by the volume of the bay encompassed between the MHHW and MLLW surfaces. More generally, the tidal prism for any given tide is the difference between the volumes at High Water (HW) and Low Water (LW). The tidal prism may then be compared to the total volume of the bay. Wang et al. (1998) used a numerical model to estimate the mean volume of the bay as 279×10^6 m^3 or 0.279 km^3. The volume of the tidal prism on a very large spring tide is then 120×10^6 m^3 (43 percent of mean total bay volume), while the tidal prism on a very small neap tide is only 8×10^6 m^3 (3 percent of mean total bay volume). The tidal prism may also be approximated by multiplying the bay area (44.3×10^6 m^2; Peeling 1975) by the tidal range. Taking the greater diurnal range (1.72 m) at TG0 as typical, the tidal prism volume is 76.2×10^6 m^3 or 27 percent of the mean volume. Of the total area of the bay, about 5.6×10^6 m^2 (12.6 percent) is intertidal (i.e., has a bed depth between MLLW and MHHW; IRC 1980). Finally, it is useful to put the cooling-water intake volume of the SBPP in the context of tidal processes. The maximum intake volume of the SBPP with all

four generation units in operation is 2.275 x 10^6 m^3; this is 0.8 percent of mean total bay volume and 3 percent of the daily tidal prism.

The order of the tides on the larger spring tides is such that the lower-low water directly follows higher-high water. This order of tide causes the falling tide after higher high water (the greater ebb) to have stronger currents than either the preceding or following flood. This predominance of fall over rise increases with increasing tidal range. This situation is typical of most West Coast bays. It may be an important factor, along with a somewhat limited sediment supply, in maintaining the bed of most of south bay in a subtidal state. Further tidal properties are described in **Section 4**.

2.6 Human Alterations

San Diego Bay is bordered by a metropolitan population of several million people, and it supports a large number of recreational, commercial and naval facilities and activities. The bay has undergone major changes in shape and depth associated with the development of a city on its shores. The largest changes came first, with the diversion of the San Diego River in 1852, as well as construction of jetties at the mouth, dredging of a shipping channel, and construction of docks. Shelter Island and Harbor Island marinas were dredged and the "island" shorelines armored. Particularly intensive dredging occurred during the years 1941–1945. Additional marinas and docks have been constructed throughout the twentieth century, with Coronado Cays being completed in south bay in the 1980s. The shipping channel has been deepened and now is 16.2 m deep at the mouth, 14.3 m in the outer bay (up to Naval Turning Basin, i.e., at Broadway), 12.2 m from there to the Tenth Avenue Marine Terminal, and about 10.8 m south to National City Marine Terminal. Further dredging is being considered, and the idea of a second entrance in south bay has been proposed several times.

There has been a major loss of marshlands and intertidal lands throughout San Diego Bay (Peeling 1974), with the airport and much of the Port and city having been developed on "reclaimed" salt marsh. In south bay, tidal areas have been used for salt pans and further urban/port development. Much of the bay shoreline is now armored—erosion resistant steep banks with negligible intertidal volume. The rivers running into south bay have also been contained within concrete channels and their mouths moved (e.g., the Sweetwater River). In recent years there has been growing awareness of the loss of habitat in California and San Diego. This has resulted in a number of projects, most notably the California least tern habitat developed on an island in the southernmost part of south bay, and the removal of some salt pans with restoration of these areas to viable habitat.

The water quality of San Diego Bay has also been much changed by the human activities on its banks and in the watershed. Most notably, water quality started degrading with sewage discharge in the late nineteenth century and industrial discharges in the early twentieth century. By the 1950s the bay was highly eutrophic, unhealthy, and odorous, and supported few native fauna. This was remedied beginning in the 1960s with the building of the Pt Loma outfall. Present levels of nutrients, plankton, oxygen, pH, and fecal bacteria are not considered to be problematic. However, loading of other pollutants has continued to impact the bay—notably metals such as copper and zinc and organic compounds such as TBT and PCB. Presently, state,

county, city, port, and navy agencies are working together in cleaning up the bay, but sediment contamination, spills and non-point pollution inputs remain a problem. Non-point pollution is primarily from the watershed and is delivered to the bay by rivers, e.g., Chollas Creek (Schiff et al. 2001). There is, therefore, continued concern for the ecological health of the bay.

3.0 OCEANOGRAPHIC PROCESSES RELEVANT TO LARVAL ENTRAINMENT

3.1 The San Diego Bay Physical Environment

San Diego Bay is a semi-enclosed bay covering about 57 km^2 (**Figure 5**). The bay is about 24.5 km long, with a broad inner bay (2-4 km wide) and a narrow outer bay (1-2 km wide). These two parts of the bay are demarcated by the narrow channel (about 500 m wide), immediately north of the Coronado Bridge. The inner bay, often referred to as south bay, is shallow (1-4 m deep), except where it has been dredged for navigation channels. With low relief surrounding south bay, it is exposed to the daily sea breezes. In contrast, the north bay is deep, on average 12 m, and more sheltered from winds. All significant rivers and creeks flow into the south bay, with only storm drains discharging to north bay. The mouth of the bay is about 1 km wide and aligned north-south, so that the whole bay has a crescent shape. Immediately outside the mouth, there are shoals on either side of the approach channel—a rocky, kelp-covered ridge to the west, and a smooth, sand depositional feature to the east.

San Diego Bay receives runoff from a 415 square mile watershed that stretches 50 miles east to the Laguna Mountains (Figure 6). The primary inflows to the bay are via the Sweetwater and Otay rivers that enter the southern reaches of south bay.

3.2 San Diego Bay as a "Mediterranean" Estuary

The climate of the San Diego region is Mediterranean, with annual rainfall of only about 0.25 m, which falls primarily during winter. Evaporation exceeds precipitation during spring, summer, and fall, with an annual evaporation of about 1.6 m (Lenz 1976). Summers are long and dry, and only following winter rain events is there any significant inflow to the bay. For much of the year, daily sea breezes dominate the wind patterns, with afternoon speeds exceeding $5ms^{-1}$ over south bay in summer. So, while the bay may function briefly as a classical estuary in winter, for most of the year it is a "low-inflow estuary." During the dry summers it becomes hypersaline—a pattern characteristic of "Mediterranean estuaries", as described by Largier et al. (1997). This hypersalinity is illustrated by data obtained in August 1993 (**Figure 7**).

Coastal waters are characterized by thermal stratification, which extends into the outer bay. In mid/outer bay, one can see a strong longitudinal increase in water temperature and a slow increase in salinity, resulting in a decrease in density of the water (sigma-t). While the inner bay is isothermal, the salinity continues to increase as one moves into older waters in the inner bay, resulting in an inverse density gradient. Other CTD surveys of the bay in spring-summer-fall illustrate a similar pattern.

This pattern in San Diego Bay and comparable low-inflow estuaries has been recognized by Largier et al. (1996, 1997) and is summarized in a schematic of the longitudinal zones (**Figure 8**). The outermost zone of the bay is marine in character, being flushed every tidal cycle by coastal ocean waters. The extent of this *marine zone* is scaled by the tidal excursion, which varies between 2 km during neap tides and 6 km during spring tides. These waters are typically the coolest in the bay. Beyond the immediate reach of tidal inflow of coastal waters, water may remain within the shallow bay and warm up, resulting in a zone in which there is a marked thermal gradient. This *thermal zone* exhibits vertical stratification and weak current shear associated with the longitudinal density gradient due to the thermal gradient. This "thermal estuary" circulation enhances longitudinal exchange in the outer parts of the bay and, in the case of San Diego Bay, extends beyond the Narrows so that some thermal structure is observed in the northern parts of south bay. As one moves even further into the bay and encounters even older waters (greater than about 10 days), the temperature no longer increases, but a marked increase in salinity can be observed due to the effect of evaporation. With residence times of a few weeks, evaporation can lead to a hypersalinity of a few parts per thousand above ambient seawater (typically less than 10 percent in small bays like San Diego Bay). This *hypersaline zone* is thus characterized by a longitudinal salinity gradient and a reversed longitudinal density gradient. The density minimum at the boundary between the thermal and hypersaline zones is typically found in south bay and during summer the southern parts of south bay are characterized by a weak inverse estuary structure (**Figures 7 and 9**). Finally, while there is no *riverine zone* in San Diego Bay during the dry summers, in some bays there may be a small freshwater inflow and estuarine circulation in small inflow channels.

The extent of these longitudinal zones varies with changes in tide, ocean density, and river inflow – e.g., the marine zone extends in as far as Harbor Island during spring tides and the riverine zone, absent in summer, may extend throughout the bay following heavy rains in winter.

Although these zones present a clear picture of longitudinal structure in the bay, the associated density structure influences but does not control longitudinal exchange. Preliminary analyses indicate that tidal and wind-driven circulation in south bay are far more important than any weak vertical circulation associated with hypersalinity and inverse estuary effects (**Figure 7**). Thus, while there is some speculation that the density minimum in mid-bay and the juxtaposition of classical and inverse density-driven circulation may result in a "thermohaline bar" and reduced longitudinal exchange (cf., thermal bars in lakes associated with the density minimum at 4^{o}C), this is unlikely to be important in the case of a broad wind-exposed tidal bay, like San Diego Bay. This longitudinal temperature-salinity pattern is best understood as reflecting underlying process—it is a symptom of what is happening in the bay, and not the driving force for longitudinal exchange.

3.3 Seasonality

The temperature and salinity of the bay waters vary seasonally in response to seasonal patterns in rainfall (**Figure 10**), surface heating, ocean waters, and winds. The salinity cycle is weak, with a mild increase from ambient ocean salinities during summer and fall (values of up to 36 being observed in southern extremities of south bay, as compared with 33 in coastal waters). During winter, however, there are events that may reduce salinity in south bay to less than 30

(Schiff et al. 2001), but seldom less than 20. Large drops in salinity last no more than a few days. Thus, even in winter, there are extended dry periods during which bay water salinity is similar to that of the coastal waters.

The seasonal temperature cycle is more marked, specifically in south bay (**Figure 11**). In winter, the bay is isothermal and cold (e.g., days 97–101) or there may be a significant thermal gradient (e.g., days 83–85), as in summer. During summer, the longitudinal thermal gradient varies on time scale of synoptic weather forcing, with cold waters being observed at the mouth of the bay for days at a time (e.g., days 179–182). Strong tidal variability is observed in the outer bay, where large spatial gradients in temperature are advected by strong tidal currents. This pattern is much weaker in the inner south bay, with day-night variability dominating tidal variability. By mid-summer (end of June), south bay waters may be as warm as 27^{o} C (e.g., days 174–177). Similar results are obtained from data available from initial monitoring sites maintained by the Port of San Diego (www.portofsandiego.org), with weekly averages of 15–20^{o} C in the outer bay and 20–25^{o} C or greater in the inner bay.

3.4 Dispersion Processes

A major question concerning entrainment of larvae in the SBPP intake flow at the southern end of south bay is the degree to which it entrains water from distances away from the intake. This is a question of longitudinal dispersion—how quickly waters mix along the axis of the bay. Largier et al. (1997) have made estimates of longitudinal tidal diffusivity K_H and the mechanisms contributing to K_H from observations of a steady salinity pattern during summer (**Figure 12a, b**). However, this bay-wide view does not fully resolve along-bay variations in K_H.

This problem was further addressed by Chadwick and Largier (1999a). In the outer bay, tidal pumping results in large tidal diffusivity and a rapid exchange between bay and ocean waters. This process of tidal pumping has been described and quantified in papers by Chadwick and Largier (1999a, b). Tidal pumping is also significant in the vicinity of the Narrows between south bay and the outer bay, due to the marked changes in width. This local increase in tidal diffusivity is seen in the calculations of Chadwick and Largier (Largier 1995) and ensures a robust exchange between the inner and outer parts of the bay. It is also seen in the dispersion of drifters deployed by George and Largier (1996) in the vicinity of the Narrows, and in the calculations presented below.

As one moves into south bay, however, the bay widens and tidal velocities weaken, resulting in a reduction in longitudinal mixing through tidal dispersion. Although a large volume of water moves through a cross-section during any tidal cycle, the effect of this tidal flow is limited as the tidal exchange ratio (TER) is low – i.e., the water that flows in during the flood tide is much the same as the water that flows out on the ebb tide (the ratio of new water is very low). Chadwick et al. (1995) found, for example, a TER on the order of 5 percent. But, while estimates of tidal mixing are low, there has been little careful study of tidal residual circulation and wind-driven circulation in the broad, shallow south bay. Preliminary work, based on TRIM modeling of circulation in south bay (http://sdbay.sdsc.edu/html/modeling2.html and DiBacco et al. 2001), indicates that tidal residual circulation is limited. There is no published work relating to the effect of the diurnal sea-breeze wind forcing, but Gutierrez and Winant (in press) have

shown that this can be very important in similar bays, like Laguna San Ignacio in Baja California. Nevertheless, the bulk diffusivity estimates of Largier et al. (1997) are robust (for the period of observation) as they are based on observations of hypersalinity, irrespective of mechanism for exchange. At distances more than a tidal excursion from the tidal pumping effects of the Narrows, laterally averaged longitudinal diffusivity values within south bay are no more than 20 $m^2 s^{-1}$ on a sectionally averaged basis (**Figure 12a, b**)—indicating weak longitudinal mixing.

A somewhat different situation exists during the brief runoff and salinity stratification events in winter. Vertical density-driven circulation in south bay may result in stronger longitudinal mixing, and thus flushing of south bay waters. However, in the absence of published studies of these events, it is not possible to quantify the importance of these stratification events. Recent studies indicate that these infrequent events enhance longitudinal exchange for just a day or two in the shallow backwaters of Mission Bay. These events are, therefore, of secondary importance in evaluating the general problem of longitudinal dispersion for San Diego Bay.

Understanding which waters are pumped into the SBPP would require detailed numerical and field investigations. However, a length scale L for the extent of the SBPP influence can be obtained by assuming a longitudinal diffusivity $K_H = 20\ m^2 s^{-1}$ and a planktonic larval duration (PLD) of 7 days—in this case $L \sim (K_H * T)^{0.5} \sim 3.5$ km. Under these assumptions, only plankton that started within 3.5 km of the power plant (about ¼ of south bay length) would be likely to be mixed to the SBPP intake at the southernmost end of the bay before recruitment. For larvae in the water column for longer periods and/or subject to stronger tides (and thus greater K_H), the length scale would be greater—comparable with the size of south bay. Of course, the real physical picture is complex and topography dependent. Larval behavior may also alter the length scale.

3.5 Residence Times

The spatial extent of the impacts of the SBPP intake flow on planktonic larvae in San Diego Bay is a function of the relative time scales of larvae and circulation. The larval time scale is the PLD, i.e., the length of time larvae are adrift within the water column—which varies with different species. The circulation time scale is the residence time (R_T) (i.e., the length of time water remains resident within a specified portion of the bay—which is a function of seasons and the specific weather patterns occurring in each season). R_T may be defined in a variety of ways, e.g., in the presentation of results of the TRIM model (Wang et al. 1998) at http://sdbay.sdsc.edu/ html/modeling2.html, where R_T is defined as the time it takes for 50 percent of the volume of a specific part of the bay to be replaced with ocean water (**Figure 13**). This is a similar concept to the residence times calculated from salinity distributions during the steady hypersaline period in late summer (**Figure 12**, from Largier et al. 1997)—with the innermost parts of south bay exhibiting residence times of the order of a month. Chadwick et al. (1995) also obtain a residence time of about a month, using estimates of tidal prism and tidal exchange ratio at the narrows.

While these results provide a useful illustration of which parts of the bay exhibit long residence, the time scale for this larval entrainment problem is related to the dispersion in the vicinity of the power plant. Are waters resident within a 2.5 km zone for a period of a week? In Mission Bay, a small-scale dye dispersion study found that it took >9 days to obtain a 10-fold dilution of waters at the head of the bay(Roughan et al. in prep). Similar "flushing times" may pertain for the innermost portions of south bay, but such dye dispersion studies have not been carried out here. Instead, we rely upon estimates of large-scale dispersion to define the source volume from which larvae may be entrained.

3.6 Definition of a "Source Volume" for the SBPP

The problem of larval entrainment versus dispersion can be expressed as a ratio of volumes, or time scales, but it is really a question of rates—entrainment rate versus dispersion rate. This has been explored previously by Largier (2001), who compared expressions for larval concentration with and without entrainment in the case of Morro Bay. Here in San Diego Bay, the intake is at the head of the bay and entrainment rate can be compared with dispersion rates (longitudinal mixing toward or away from the intake). There are several relevant cases:

- Localized population: For a localized population (i.e., one that spawns into a volume smaller than $Q_{pump*}PLD$), the stronger the dispersion (the larger K_H) the more larvae are excluded from entrainment. For $K_H = 0$, all larvae within the volume $Q_{pump*}PLD$ are entrained, but no larvae outside this volume are affected. Knowledge of K_H near the intake flow is vital for such species.
- Widespread population: For a widespread population (that is homogeneously distributed throughout all of south bay or a larger volume by strong dispersion), the exact value of K_H is irrelevant in the absence of an intake flow, because larvae that disperse away are replaced by others being dispersed towards the intake. In the presence of an intake flow and if the larval entrainment is significant enough to reduce local larval concentrations, then it will create a localized larval concentration gradient indicative of larval entrainment, and the value of K_H again becomes relevant. If the larval entrainment is small relative to other processes, no gradient is seen, and the exact value of K_H remains unimportant.
- Local absence: For a population absent from the local region, but nearby, the larger K_H, the more larvae that are brought into the intake zone. For zero dispersion, none are entrained. In this case, K_H throughout all of south bay is highly relevant.

Different larval populations may exemplify different cases, and the same population may evolve from one case to another over time, rendering very difficult practical estimates of the impacts of an intake flow. Thus, many approaches to assessing the impact of larval entrainment are based on the idea of a specific source volume (a concept adopted from analyses of closed water bodies). Here and in Section 4, we seek to define a source volume for San Diego Bay larvae. The source volume is best thought of as the volume of water into which larvae are mixed over their planktonic life stage or stages (the PLD)—this is the idea of a "larval pool". And, if this volume intersects with the power plant intake, then some of these larvae will be entrained. The proportional larval loss is then the number of larvae entrained (evaluated empirically),

divided by the total number of larvae in this "source volume" or "larval pool". If there are inadequate data on intake concentrations, then the number of larvae entrained can be obtained by considering what fraction of the source volume is entrained during the PLD, given the intake flow rate Q_{pump}.

While it is in principle desirable to carry out calculations for individual species (identifying adult/spawner distributions and PLD for each species of concern), there is often a desire for more general results that provide straightforward policy direction. Here we focus on the oceanographic background relevant to generalized calculations for organisms with PLD longer than a week. For these longer time scales, and for a longitudinal diffusivity of ~20 m^2 s^{-1} or greater, one can expect larvae to be mixed readily over distances of several kilometers, comparable with the size of south bay. With the possibility of enhanced mixing due to wind forcing and/or the influence of larval behavior, we suggest using the well-defined south bay (up to the Coronado Narrows) as the source volume for all populations with PLD of the order of a week to a month. This approach is consistent with estimates of residence time discussed above, and the expectation that the internal mixing time of south bay is between a week and a month. For longer PLD, the flux of larvae through the Narrows should be taken into account and the source volume becomes more difficult to define. For shorter PLD, the source volume is smaller and more local to the vicinity of power plant—and the detail of flow patterns becomes important. For this localized problem (small PLD, small K_H), even though the population impact may be small (only a small portion of the bay population will be entrained), the local community impact may be quite high. This is a special case that goes beyond the source volume approach to assessing the impact of larval entrainment.

The following section documents tidal processes and values of K_H determined from analyses of tidal currents. These processes and K_H values are pertinent to establishment of a source volume in several respects. First, they define the tidal elevations necessary to definition of any source volume. Second, they show that south bay is a distinct body with (in effect) a mouth at the Coronado Narrows. Finally, they provide detailed confirmation of results of the earlier studies of tidal dispersion described in **Section 3.4**. Given the estimated tidal dispersion levels, south bay as a whole is expected to be the relevant source volume for PLD values of about a week to a month.

4.0 TIDES, CURRENTS AND TIDAL DISPERSION

Tides are a major factor in the ecosystem of U.S. West-Coast estuaries. Tidal measurements provide, moreover, vital information regarding physical oceanographic and ecosystem characteristics. In this regard, measurements of surface elevation are a powerful tool, because they allow the broad patterns of tidal processes to be readily discerned. Typically, tidal elevations and properties like tidal range have large physical scales (relative to estuary length and width) and change only slowly along an embayment. Also, the spatial pattern of tidal range and tidal datum levels must be determined, because the source volume has been defined as the volume of south bay below Mean Water Level (MWL), an important tidal datum level.[1] Tidal

[1] The total source volume is the sum of the subtidal volume (volume below MLLW) plus the volume between MLLW and MWL, both for the estuarine surface area south of the Coronado Narrows. The estuarine surface area is the area encompassed within the estuarine shoreline. This definition excludes areas like the salt ponds around the

and mean currents play an important role in the flushing of pollutants and in larval dispersion. We have, therefore, documented patterns of tidal and mean currents and calculated dispersion due to a variety of tidal processes.

4.1 Data Sources

4.1.1 Surface Elevation Data

Surface elevation measurements have been made over the last 20 years at several locations in San Diego Bay providing a good basis for understanding tidal processes; see **Figure 14** and **Table 1** for station locations. There is, moreover, a National Oceanic and Atmospheric Administration (NOAA) San Diego Bay reference station in north bay; the San Diego Bay station or TG0 in **Table 1**. This station has been maintained continuously since 1907, providing insight into long-term trends in sea level and tidal range. Outside San Diego Bay itself, the gauge at La Jolla has been maintained since 1924, documenting trends in ocean tidal characteristics. NOAA records indicate that tides were observed from 1970 to 1983 at Ballast Pt., but only a short segment of this record from 1983 has been digitized and made available to the public. Of the remaining gauges listed in **Table 1**, only the Broadway (TG2) and south bay (SB) stations have records extending a year or more. The Broadway station essentially duplicates the main San Diego Bay station. Station SB has data scattered over almost a two-year period (fall 1993–summer 1995), but gaps increase toward the end of the deployment period. The first year of the record has relatively continuous data and has been used here; half hourly samples were used for harmonic analysis purposes. The 1983 National Ocean Survey-NOAA (NOS-NOAA) stations have a month or less of hourly data. Some NOS stations exhibit gaps in coverage.

With one exception, all of the tidal records used here are either from surface tidal gauges or compensated benthic pressure gauges and are, therefore, unaffected by atmospheric pressure fluctuations. The remaining gauge (Station OS200) is an Ocean Sensors model 200 CTD, which uses an uncompensated pressure gauge. Atmospheric pressure fluctuations modify the low-frequency portion of tidal records collected by such instruments, but this has little or no impact on the tidal properties here determined from this record. The OS200 record was two months in length, during summer 1993. Half-hourly samples were employed for harmonic analysis.

4.1.1 Current Meter Records

We employ here records from three types of current meters to define spatial patterns of tidal and mean currents (also known as non-tidal or residual currents) in south bay (**Figure 14** and **Table 2**). Current data were collected by NOS in 1983 using Aanderaa current meters. These meters count revolutions of a rotor over time to measure current, averaged over a sample period. Direction is determined once per sample period using a large vane. Aanderaa meters can give erroneous results if the meter is subjected to large waves, which inflate the rotation count. Because the vane cannot follow the rapid changes in current direction and because direction is

mouth of the Otay River that, while low enough to be inundated, are excluded from daily tidal inundation by dikes. MWL is the average water level over a lengthy period of time, ideally several years. It is similar in concept to Mean Sea Level (MSL), but MSL can only be determined from a record of at least 18.6 years length.

sampled infrequently, direction measurements also become meaningless in the presence of large waves. South bay is well protected from ocean waves, and the small surface waves that do form (up to 2 ft) do not penetrate deeply enough into the water column to affect the NOS records. These records are, therefore, of high quality, though there are gaps in some records. The Aanderaa current meters were set to record 10 min intervals, and the data were used in this form (without filtering or decimation) for harmonic analysis and dispersion calculations.

Endeco current meters (Model 174SSM) were employed at three locations (A24, A28, and A41) during the summer of 1993, then again during the following winter (Wang et al. 1998). Only the summer records were used here. While the Endeco meters employ a more advanced rotor system than the Aanderaa current meter and were not at all affected by wave action, they were quite susceptible to biofouling. Care was required, therefore, in the selection of data used for harmonic analysis. Portions of these records that exhibited long periods of low or zero velocity were excluded. Records were also truncated when there was a systematic decrease in the ratio of currents to surface elevation (judged using data from or predictions for the San Diego gauge). The Endeco meters were set to record data at 2-minute intervals. The 2-minute samples were filtered (using a simple triangular filter) and decimated to half-hourly intervals for harmonic analysis and dispersion calculations.

The final type of instrument used to measure south bay currents was a narrow-band acoustic Doppler current profiler (NB-ADCP) manufactured by RD Instruments (station NB2). These acoustic instruments measure the Doppler shift of sound reflected from ambient particles in the water to determine velocity. A complete profile of currents is produced at each sampling interval. This profile is discretized into "bins" that reflect the frequency of the instrument used. Low frequencies (with long wavelengths and large bins) are used in deep water to optimize the total depth that can be sampled, while higher frequencies (with shorter wavelengths and smaller bins) are employed in shallow water, to optimize the resolution over a short water column. One-meter bins were used in the present instance, so that detailed current profiles could be measured in ~12 m of water. ADCP records are normally not affected by either biofouling or (with sufficient averaging) by surface waves. The single record from summer 1993 is more than two months long and of high quality. No gaps were noted and no data editing was required. The NB-ADCP was set to record data at 6-minute intervals. The 6-minute samples were filtered (using a simple triangular filter) and decimated to half-hourly intervals for harmonic analysis and dispersion calculations.

4.2 Data Analysis Methods

4.2.1 Harmonic Analysis of Surface Elevation and Current Records

The determination of tidal and mean flow characteristics from surface elevation and current meter records was carried out using a harmonic analysis program called t-tide (Pawlowicz 2002), written in the Matlab language. The t-tide program is based on Godin (1972) and the Foreman (1977, 1978) Fortran codes (which used separate but similar codes for tides and currents). The t-tide code is able to analyze both tides and two-dimensional (in the horizontal) current vectors using a single code by treating the current vectors as complex number (with a real and imaginary part). The Foreman programs were considered the standard in North America for

tidal analysis for more than two decades. The choice of the newer t-tide program is dictated by its superior error analysis and ease of use. Since issuance of t-tide, Dr. Foreman has ceased to support the older Fortran routines.

For tidal heights, t-tide provides estimates of tidal amplitude and phase for the major tidal constituents, plus the mean elevation and trend of the data (if needed). The phase is the number of hours high water occurs after the passage of the moon over the local meridian.[2] These constituents are a convenient apparatus used to describe the complex but nearly deterministic time variations of the major once-daily (diurnal) and twice-daily (semidiurnal) tidal waves. These tidal waves are fundamentally related to astronomical forcing. Estimates are also provided for constituents in "overtide" species. Overtide constituents occur at frequencies higher than those of the major tidal species and are sums and differences of the basic tidal frequencies within the major species. Most overtide energy in an embayment is not the result of astronomical forcing. It arises instead from the effects of friction and wave distortion on the diurnal and semidiurnal tide, as induced by shallow bed depths. Because overtides are fundamentally a property of an estuary, they vary more rapidly throughout an embayment than is the case for the major species. The character of this variation is an important indicator of estuarine processes and may give rise to both larval transport and dispersion.

For tidal currents, t-tide describes the rotation of the tidal currents over the tidal cycle in terms of an ellipse. The parameters estimated include major and minor axis amplitudes, ellipse orientation and phase. The major axis amplitude corresponds to the speed at the time of peak flood or ebb. In a channel, it will typically be oriented more or less along the channel. The minor axis amplitude corresponds to the peak speed normal to the major axis at the change of the tide. For essentially reversing tides in a channel, the minor axis amplitude is nearly zero. Over or near tidal flats, however, the amplitudes of the major and minor amplitudes may be similar, such that the current rotates around what is almost a circle; this is often also the case in open coastal waters. A tidal current ellipse is also characterized by an orientation (direction of the major axis) and a phase (the time at which the current is in the direction of the major axis). The direction of the major axis is, by convention, always in a northerly direction (i.e., between -90º and +90º True). Depending on channel orientation, this convention does not always give the flood direction as one might expect; indeed the direction of flood is a local navigational convention that often does not have any simple mathematical definition. The ellipse orientation may, however, be reversed by 180º to conform to local convention and physical reality. This also changes the phase by 180º. Mean flows (the average after removal of the tides) are described in terms of {u,v} components, or alternatively in terms of mean speed and direction.

Duration is an important characteristic of a tidal record. Tidal properties are somewhat variable over time, though typically less so than for other oceanographic properties. A complete tidal description requires 18.6 years of data, but one year of data is sufficient to describe the tides with sufficient accuracy for most purposes.[3] Moreover, t-tide uses a technique called inference,

[2] More formally, each of the more than 400 tidal constituents is described in terms of an imaginary satellite that would provide the tidal forcing described by the constituent in question. The sum of all of the forcing from all these satellites yields the complex gravitational forcing provided by the interaction of the sun, moon, and earth.

[3] Much of the difference between a 1-yr record and an 18.6-yr record can be compensated using "nodal modulation", which accounts for the typical behavior of certain small constituents; t-tide uses nodal modulation.

such that a lengthy (1 yr) record is needed in only one location in an embayment or region. Inference uses the fact that the amplitude ratios and phase differences amongst closely spaced frequencies change more slowly than the behavior of the major constituent within the group of closely-spaced constituents. This technique is quite important in the present situation, in that many current records are ~20 days duration. Tidal records (aside from stations TG0 and SB) are mostly ~1 mo in duration. The amplitude ratios and phase differences within the diurnal and semidiurnal tidal species as determined at the NOAA reference station (TG0) were used for inference for all current and surface elevation records throughout the bay. For records <600 hrs, the semidiurnal constituents N_2 and K_2 were inferred from M_2 and S_2, respectively. For other records <~6 mo, only K_2 needed to be inferred, because N_2 could be determined directly. The diurnal constituent P_1 was inferred from K_1 for all records <6 mo. Through the use of t-tide with inference then, tidal estimates have been formed that reasonably reflect typical tidal behavior in San Diego Bay.

Duration also determines how many constituents can be used to describe the complex though largely stationary (in the statistical sense) tidal variability in San Diego Bay. There are >400 constituents that are within a factor of 10^{-5} as strong as the dominant lunar semidiurnal (M_2). Fortunately, most of these are quite small ($<10^{-3}$ as large as the largest constituents). A yearly record allows analysis of 60-70 constituents, including overtides. A one month record allows consideration of 30-40 (again depending on the overtides chosen), while only 15 are available from a two-week record. Fortunately, the presence of the long-term reference station at San Diego (TG0) and the use of inference still allows robust analyses to be carried out that capture most of the tidal variance.

Two methods of error analysis are built into t-tide (Pawlowicz et al.2002): a) a linearized analysis of the residual spectrum (after removal of the tidal signal), and b) a fully nonlinear parametric bootstrap approach. In the latter, residual variance estimates are used to simulate a number of replications of the analysis, based on the tidal amplitudes and added Gaussian noise. The second approach was used here to provide 95 percent confidence limits; a signal-to-noise ratio (SNR) is also provided in t-tide output. For the major constituents reported here, SNR is typically high (10 to >1000), though the K_1 SNR was ~4 at buoy 41, because of the low current velocities. It is also typically found that the directional uncertainty is the largest limitation in using tidal current analysis results, where amplitudes are determined with reasonable certainty except for the smallest constituents. This corresponds to real sensor limitations—current meter compasses are usually not accurate to better than about 5º.

There are two basic methods for determination of tidal datum levels—averaging of the relevant tidal elevations for long periods of time, and use of formulae that specify datum levels in terms of harmonic constants (U.S. Coast and Geodetic Survey 1952). The accuracy of either approach can be improved through comparison of results from individual tide gauges (having limited lengths of deployment) to established results for a nearby, long-term reference station. We have employed the second method, correcting the raw results for each gauge using the NOAA reference station at San Diego Bay (TG0). Thus for example, tidal range estimates were made with the harmonic formulae for TG0 for observation periods that matched the period of observation for each of the other gauges. The raw range estimate for each of the other gauges

was then multiplied by a ratio of ranges (*Ratio*) at TG0; *Ratio* = long-term range at TG0/range at TG0 for the specific observation period.

4.2.2 Estimates of Tidal Dispersion

Larvae are transported or dispersed by both mean and tidal currents. The mean currents may be vertically and horizontally sheared, such that the fate of larvae depends on their location in the water column. While tidal currents are reversing, they may still transport larvae through a variety of dispersion processes. Tidal dispersion is analogous to horizontal turbulent diffusion. Because, however, tidal dispersion is calculated as the net result over a tidal cycle (much longer than the averaging time for turbulence), and because tidal currents are an order of magnitude greater than turbulent fluctuations, tidal dispersion is typically much larger than turbulent diffusion. It is important to realize, however, that the process of tidal dispersion is the result of viewing a system in a tidal average sense—if tidal motions could be resolved every few minutes throughout south bay down to the scale of a few meters (e.g., by remote sensing or in some sort of ideal computer model), then all scalar transport could be directly resolved, and there would be no need for the concept of tidal dispersion. Only turbulent diffusion would then need to be considered. Such a theoretical exercise is well beyond present computing and observational capabilities. Therefore, larval transport due both to tidal dispersion and mean flows needs to be considered. We find below that mean currents are quite small and spatially variable; tidal dispersion plays, therefore, a dominant role in larval motion. The spatial pattern of tidal dispersion is accordingly a major consideration in defining south bay source volume boundaries.

There are a variety of processes that may lead to tidal dispersion, as noted in **Section 3**. The importance of the overall process of tidal dispersion typically varies smoothly along the length of an estuary (e.g., **Figure 12**), but topography may cause localized variations in the importance of individual mechanisms; this feature is reflected in the results below. Three longitudinal tidal dispersion mechanisms are analyzed here, based on inspection of the current meter data, physical reasoning, and the earlier studies described in **Section 3**. For each of these mechanisms, the strength of longitudinal tidal dispersion is characterized in terms of a "dispersion coefficient" K_H, which has units of m^2s^{-1}. In scaling terms, K_H is the product of a characteristic horizontal velocity (a current speed with units of ms^{-1}) and a length scale (e.g., a tidal excursion or channel width with units of m). The larger the scale of the motion and the stronger the currents associated with it, the stronger the dispersion.

The three tidal dispersion mechanisms calculated from the available current meter data set are:[4]

- Tidal dispersion due to streamline curvature K_{HR}: This form of dispersion occurs when flood and ebb currents at a location are not aligned 180º opposite one another or with the

[4] The vertical and horizontal pumping and trapping mechanisms estimated by Largier et al. (1995) from vessel data are not considered here because they are not important in south bay, and could not be calculated directly from the current meter data available. Current meter data provide temporal coverage that is superior to that of vessel data, but at the cost that not all mechanisms can be considered. Because larvae persist in the system for substantial periods, improved temporal coverage was considered to be the dominant consideration.

mean flow. It is expected to be very strong when there is a small radius of channel curvature R, a circumstance not present in most parts of South Bay. It may also be important, however, in areas where channel width changes rapidly, a circumstance seen in several locations in South Bay. This curvature causes motion normal to the mean axis of the tidal motion (the average direction between flood and ebb). Because along-channel currents are also laterally variable, this form of lateral dispersion can exhibit a strong influence on larval fate in some locations. If only M_2 tidal currents are present, then the normal motion is seen in the mean flow and in the M_4 current ellipse. For a mixed tide as in San Diego Bay, normal motion occurs at a variety of frequencies, and it is more straightforward to estimate this form of dispersion from the original current meter data rather than harmonic analysis results. By analogy to the skew dispersion formulation of Fischer et al. (1979), we estimate:

$$K_{HR} = H^2 / K_m \{U'V'\} \quad (1)$$

where: K_m is the vertical turbulent eddy diffusivity (obtained by a standard formula for neutrally stratified flows), H is depth, and the braces { } indicate a tidal cycle (12.5 hr) average. U' and V' are the currents along and normal to (respectively) the axis of the M_2 tidal current. When this axis deviates from the actual direction of the channel or mean flow, then substantial, though local, tidal dispersion occurs.

- Tidal dispersion due to lateral shear K_{HL}: This form of dispersion is caused by lateral turbulent mixing across a channel. If there is no streamline curvature, $K_{HL} > K_{HR}$; even a small streamline curvature, however, causes K_{HR} to predominate. Fischer et al. (1979) suggest:

$$K_{HL} = 0.02 * factor \{U'U'\} T \quad (2)$$

where: *factor* is a function of the ratio of tidal period T to cross-channel mixing time scale. Note that the presence of streamline curvature speeds up cross-channel mixing, which then decreases *factor* and K_{HL}. The K_{HL} and K_{HR} estimates tend, therefore, to vary inversely to one another.

- Tidal dispersion due to vertical shear K_{HV}: This form of dispersion is caused by vertical turbulent mixing over the depth of a channel. In strongly sheared channel flows, it is an important mechanism, but may be inhibited by the presence of strong vertical density stratification. For this mechanism acting in a neutrally stratified flow, Bowden (1983) suggests:

$$K_{HV} = 0.033 H^2 / K_m \{U'U'\} \quad (3)$$

For each of the above three mechanisms, the K_H estimate is formed by averaging over a tidal day of 12.5 hours, using the available data for each current meter. This resolves the tidal-daily variation in tidal dispersion. On the other hand, R_T is of the order of weeks in South Bay. Thus, salinity and larval distributions may be expected to reflect the time-average dispersion over R_T or the PLD, respectively. It is also important to note that the estimates formed below from tidal current data are fundamentally local, and are affected by the fine-grained nature of estuarine current variability. They have the advantage over the estimates of **Figures 12a, b** of giving an idea of the time variations of dispersion processes, but the estimates of **Figures 12a, b** (which are based on the salinity distribution) are more integrative, in time and space.

K_H should, moreover, be viewed as a measure of the potential importance of dispersion. For any property P, the actual dispersion is the product $K_H \partial P/\partial s$ of K_H with the spatial gradient $\partial P/\partial s$ in the local longitudinal direction s (the direction of s being defined as along the axis of the local M_2 tidal current U). If the local gradient vanishes ($\partial P/\partial s = 0$) then there will be no net transport, no matter how large K_H is. The actual importance of tidal dispersion is, moreover, a function of the property considered. While biological properties like larval populations are strongly influenced by physical properties like salinity gradients, there is no guarantee that larval and physical attributes (e.g., salinity) will be affected in the same way by tidal dispersion, because their gradients may be of different strength, even when they occur in the same general location. Finally, larval behavior may cause larval tidal dispersion to be fundamentally different from dispersion of physical properties, especially if vertical migration is coordinated with local current strength.

Current meter record length is also important in the context of defining mean flows and dispersion relationships. Tidal currents are strongly variable over the tidal day and tidal month. They are not strongly variable on a seasonal basis, though subtle differences emerge through the influence of density stratification and tidal-mean flow interactions, which may be expected to somewhat affect K_H. Nonetheless, tidal dispersion estimates are not expected to be strongly variable from season to season. In contrast, mean flows in San Diego Bay do vary substantially from season to season. While such flows in this system are typically small, their relative variations are still substantial. Available data do not allow a characterization of this seasonal variability.

Uncertainty estimates for K_H are of some importance, but difficult to define because the most important uncertainties are systematic, not random. K_H varies between the two tides of a day and over the tidal month. Adequate data exist within each tidal day (25 and 75 points, for Δt = 30 and 10 minutes, respectively) to resolve the tidal variations and average any random errors in individual data points. Adjacent estimates may be combined to reduce the random error for any tidal phase (e.g., neap or spring tides). In some cases, several neap and spring tides may be averaged together to characterize these conditions, also. The following systematic uncertainty sources should be considered:

- Definitional: Different authors have used different conventions (especially different constants) that can cause 50-100% changes in the various K_H modes. This form of uncertainty is of relatively small importance for present purposes, however, because we are interested in spatial patterns and estimates for each component of K_H have been applied consistently to all stations.

- Spatial variability: The estimates formed from individual current meters are a function of local currents, which vary substantially across and along the estuary. Considerable station-to-station variability is seen below that likely does not reflect cross-sectional average conditions.

- Selected Mechanisms: Not all tidal dispersion mechanisms can be calculated from the current meter data set, though the three that have been estimated are believed to be

dominant in South Bay. **Figure 12b** suggests that tidal pumping mechanisms may be dominant on the seaward side of the Narrows and close to the estuary mouth. Tidal trapping may be locally important at various locations, but it is not thought to be globally important. The K_{HR} term may also capture some of the tidal trapping effect documented by Largier (1995). Similarly, we have not treated dispersion to wind-driven circulation, which was also not explicitly considered by Largier (1995). However, winds may well account for some of the dispersion considered here as part of the K_{HR} term.

- Tidal cycle duration: The average duration of a tidal cycle is 12.42 hours, which is slightly aliased by use of 12.5 hours of data for each estimate. The resulting average relative uncertainty is small (of O(0.08/12.42) = 0.6 percent) and oscillates with a period of about 2.6 mo. More significant is the fact that the actual duration of individual tidal cycles is not always 12.42 hr. Instead, it varies from ~10.5-14 hrs for West Coast estuaries. The effect of using an average duration instead of the actual duration is to smear adjacent tidal cycles together, reducing the difference between successive tides during those parts of the tidal month with a large diurnal inequality (large difference between successive tides). Thus, this type of error confers a central tendency on the results and is not, therefore, a serious concern.

- Vertical mixing coefficient, K_m: The estimates of K_{HR} and K_{HV} employ a value of a vertical turbulent mixing coefficient K_m, for which a conventional estimate appropriate to a neutrally stratified flow has been used. If the flow is stratified, K_m will be over-estimated and K_{HV} and K_{HR} under-estimated. Averaged over a tidal cycle, this effect could easily cause errors of 50 percent. In the shallow water of South Bay and during the summer period for which data are available, density stratification is not expected to be systematic or persistent. Errors of this nature are likely to be isolated.

Despite all the qualifications of the previous paragraphs, the spatial distributions of mean flow and K_H are valuable indicators for determining source volume boundaries. We shall see below that the Coronado Narrows is marked by a local maximum in mean currents and tidal dispersion (confirming **Figure 12b**). In effect, the Narrows acts as the "mouth" of South Bay. It forms, therefore, a natural physical oceanographic boundary that may be used to define the seaward limit of the SBPP source volume.

4.3 Tidal Height Characteristics

The patterns of tidal height characteristics are summarized in **Tables 3 to 5**. **Table 3** lists the characteristics of the dominant diurnal (once-daily) tidal constituent K_1, while **Table 4** shows the properties of the largest semidiurnal (twice-daily) tidal constituent M_2. **Table 5** summarizes the behavior of the quarterdiurnal constituent M_4, an overtide created by the interaction of the semidiurnal wave with shallow-water topography through friction and wave-distortion.

There is little change along the length of the estuary in K_1 amplitude, whereas M_2 amplitude increases by >12 percent (**Tables 3 and 4**). Thus, the tide becomes somewhat more semidiurnal towards the landward end of South Bay as tidal range increases landward. The

amplification of M_2 but not K_1 suggests that it is resonance not convergence that is primarily responsible for the increase in tidal range in the system. Thus, the tide in San Diego Bay approaches a standing wave condition. Under these circumstances, high (or low) water occurs at the same time throughout the bay, and the tidal current leads the tidal height by ~90º. The variations along the bay in the phases of the M_2 and K_1 waves are quite small, only a few degrees, and not physically important.[5] They are, however, still statistically significant. These small phase differences may be related to local topography near the tide stations, but it is more likely that diverse sampling periods and record lengths in the data set are responsible for the observed variations. M_4 amplitudes are small throughout (**Table 5**), as is also the case with other overtides. This indicates that the friction on the tidal wave is fairly small, as a consequence of the weak freshwater input and relatively small percentage of inter-tidal bed depths. Given the small overtide amplitudes, it is difficult to interpret the M_4 phase variability—some of it is simply random, but local topographic effects may also be important.

Overall, analyses of data collected at eight tide gauges in San Diego Bay suggest that there is a moderate increase in tidal amplitude and tidal range in the more landward parts of San Diego Bay. This slight amplification (primarily of the semidiurnal wave) is consistent with the idea that tides in San Diego Bay form a standing wave, though decreasing channel cross-sections in the more landward part of the system may cause some of the observed increase in tidal amplitudes in South Bay. Given a standing wave character, it is expected that times of high and low water will change little over the length of the bay. There is also little overtide generation through friction or wave distortion, in part because shallow tidal flats and marshes do not cover a large fraction of the bay. It is also likely that human alterations of depths, channel cross-sections and shorelines has somewhat altered the tides of San Diego Bay.

4.4 Tidal Current and Mean-Flow Characteristics

The patterns of tidal current characteristics are summarized in **Tables 6–8**. **Table 6** lists the characteristics of the dominant diurnal (once-daily) constituent K_1, while **Table 7** shows the properties of the largest semidiurnal (twice-daily) constituent M_2. **Table 8** summarizes the behavior of the quarterdiurnal constituent M_4. Mean currents are summarized in **Table 9**.

The notable features of the tidal currents (**Tables 6–8**) are:

- Amplitudes: Tidal current amplitudes are maximal in the narrows and at the mouth of the bay, though some of the stations near the mouth were not included in this analysis. Amplitudes become very small toward the landward end of South Bay, only a few cms^{-1}. M_2 amplitudes are <20 cms^{-1} throughout South Bay, whereas K_1 currents are <10 cms^{-1}. Currents are also very weak at N5, located in very shallow water west of the channel. Its weak prevailing currents mark South Bay as a distinct environment, and the occurrence there of relatively fine sediments is consistent with these low currents.

[5] A 28.9º phase difference represents a change in time of high water of 1 hr for M^2, whereas for the diurnal constituents, a change of ~15º corresponds to 1 hr.

- Reversing character: The major axis amplitude is typically an order of magnitude larger than the minor axis amplitude, so the currents associated with the major tidal constituents are largely reversing not rotary.

- Direction: Currents at the three most landward stations (Buoy 41, N1, N2) are notably almost normal to the channel direction, which is NNW-SSW. These meters were located at or near turning basins where the channel is wider than elsewhere. The anomalous directions for these currents may be related to the local complex topography

- Phase: Even considering error limits and the 180º ambiguity of ellipse direction and phase, current phases are more irregular tidal height phases. This is likely because most of the available records are short, ~20 d in most cases.

- Overtides: Like M_2 currents, the M_4 currents are still mostly reversing. However, M_4 currents are quite small, <2 cms^{-1} at all locations, with irregular orientations and phases. Still, the M_4/M_2 current amplitude ratio is considerably larger at most stations than the corresponding ratio for tidal heights. These factors indicate that overtide currents are primarily driven by local complex topography and channel curvature. Examination of other overtides (not tabulated here) confirms this general picture.

Mean currents are generally weak (**Table 9**), a few cms^{-1}. Oddly, the highest mean current speed is not seen in the Narrows (the ADCP at NB2 and N8) or near the mouth (N10 and N12). Rather is at N1, near Sweetwater Creek. Here, the mean speed is >4 cms^{-1}, oriented ~140º to the left of the M2 tidal current and oblique to the channel axis (which is NNW-SSW). Clearly, the currents in this location are somewhat atypical, and this is also the case for N2 and Buoy 41. Tidal currents and the mean flow at the Narrows are much better aligned (N8 and NB2) though much weaker relative to the tidal flow. Progressive vector diagrams for N2 (tides and mean flow oblique) and NB2 (tides and mean currents aligned) provide a feel for the different character of the currents under these two circumstances (**Figure 15**).

It is also useful to provide a qualitative feel for the importance (relative to dispersion) of a mean current of 1 cms^{-1}. Over a 12.42-hr tidal cycle, a spatially uniform current of 1 cms^{-1} will carry a particle 450 m. Over 7 days, a transport of ~6 km will occur, if the mean flow were persistent in time and space. In contrast the dispersion scale for a K_H of 20 m^2s^{-1} ($L = (K_H T)^{½}$, as in Section 3.4) is 940 m for T = 12.42 hrs and ~3.5 km for 7 days. Thus, currents may potentially carry larvae farther than dispersion, if they are spatially and temporally coherent. The long residence time R_T of South Bay (typically several weeks) suggests that this is not usually the case. Moreover, mean flows are likely <1 cms^{-1} for most locations in South Bay, and the observed orientation of the means flows at the various stations is not consistently seaward. Thus, we have focused on dispersion rather than mean flows in larval dispersion.

In summary, analyses of mean and tidal currents measured at 18 locations throughout the interior of the bay show that tidal currents exhibit a local maximum in the Coronado Narrows and increase toward the mouth of the bay. Tidal currents are small in South Bay, and mean flows are modest throughout the system. These results suggest that larvae are likely removed from South Bay primarily but not exclusively by dispersion. This idea is subject to the

qualification that advection may be dominant over tidal dispersion during winter river-flow events.

4.5 Estimates of Tidal Dispersion

Tidal Dispersion estimates are summarized in **Table 10**, which provides a root-mean-square (rms) and typical neap and spring values for total K_H for each various current meter. The spatial distribution of rms total K_H is shown in **Figure 16**. The notable features of the total K_H distribution are as follows:

- Magnitude: The largest estimated total rms K_H values occur in the Coronado Narrows. South bay values of K_H decrease toward the head of the bay. K_H also increases toward the mouth, where K_H values may exceed those in the Narrows. This suggests that it is appropriate to treat the Narrows as the mouth of South Bay and define a source volume landward of this point.

- Variations with depth: Interestingly, there is no clear pattern of K_H values with depth. At some locations, K_H is larger at depth than at the surface, despite a general decrease in tidal current amplitude toward the bed. This may be the result of complex near-bed topography that affects the tides and mean flow somewhat differently.

- Neap-spring variations: While it might be expected that tidal dispersion would be maximal on spring tides when tidal currents are maximal, this is not the case—some stations show maximal K_H on springs while others have maximal K_H on neaps. The reasons for this are related to temporal variations in the individual mechanisms, as discussed below.

The time histories of K_{HR}, K_{HL}, K_{HV}, and total K_H provide important insights in dispersion mechanisms; time histories for three stations are shown in **Figure 17**. The >60 d record from the ADCP in the Narrows (at NB2) show much higher total K_H on spring tides (ca. d 183, 198, 211 and 226) than on neap tides (**Figure 17a**). K_{HL} and K_{HV} contribute strongly to total K_H, whereas K_{HR} is insignificant. This station also has the highest rms total K_H for any location analyzed. The mean and tidal currents are very well aligned here (**Figure 15**), explaining the small values of K_{HR}. Station N4 (in shallow water SE of Glorietta, **Figure 17c**) is not located in a major channel. It yielded the lowest K_{HL} values of for any station. On the other hand, Station N1 (**Figure 17c**) is typical of the three southernmost current meters in South Bay (N1, N2 and bouy41). All three meters are at or near the National City or Sweetwater turning basins, presumably because these locations were convenient for deployments. Tidal currents are almost normal to the channel, and the mean flow is oblique to both the channel and tidal flow. The result is very high local values of K_{HR}, which accounts for almost all of the total K_H. Interestingly, K_{HR} and total K_H at both N4 and N1 are maximal on neap tides (ca. d 255-260 and at d 270), apparently because the cross-flow is somewhat stronger at that time.

The results of **Figures 12a, b** suggest that the values estimated for N1 (Figure 17c) cannot be typical of South Bay as a whole—deep channels are convenient for current meter deployment but do not make up a large fraction of South Bay habitats. Results for N4, (Figure

17b) are likely more representative. In terms of mechanisms, the N4 results are similar to those for N1, in that the maximum values of K_{HR} and total K_H occur on neap tides (ca. d 242). Also, K_{HL} and K_{HV} do not contribute much to total K_H at either station. Still, the rms total K_H at N4 (7.4 m^2s^{-1}) consistent with values previously estimated (Figures 12a, b and Largier 1995).

In summary, estimates of tidal dispersion were formed using data from 18 current meters deployed throughout the interior of the bay. The spatial patterns are generally similar to those from Largier (1995), but there are differences in detail. While the measurements presented here provide superior temporal coverage, some of the mechanisms (e.g., tidal pumping) found in earlier studies to be important at and seaward of the Narrows could not be calculated here. An important feature depicted both in our results and those of Largier is, however, that tidal dispersion has a local maximum at the Coronado Narrows, consistent with the idea that the Narrows acts as the "mouth" of South Bay.

4.6 Tidal Datum Levels and Calculation of a Source Volume

4.6.1 Tidal Datum Levels

The tidal datum levels determined for the tide gauges listed in **Table 1** are summarized in **Table 11**. Parameters in Table 11 include:

- Extreme High Water (EHW), the highest tide observed over a long period, available only for TG0 and La Jolla.
- Extreme Low Water (ELW), the lowest tide observed over a long period, available only for TG0 and La Jolla.
- Mean Higher High Water (MHHW), the average of the higher high waters of each day.
- Mean Lower Low Water (MLLW), the average of the lower low waters each day.
- Mean Lower High Water (MLHW), the average of the lower high waters of each day.
- Mean Lower High Water (MHLW), the average of the higher low waters each day.
- Mean High Water (MHW), the average of all high waters.
- Mean Low Water (MLW), the average of all low waters.
- Mean Tidal Level (MTL), the average of MHW and MLW.
- Mean Water Level (MWL), the average tidal elevation over the period of record. Over a long period of time, this corresponds to Mean Sea Level (MSL).

For San Diego Bay (TG0) and La Jolla only, it is possible to determine the relationship between these tidal datum levels and North American Vertical Datum-1988 (NAVD-88).

The increases in mean and diurnal tidal range toward the landward end of South Bay are shown in Table 11 and **Figure 18**, along with MWL which is used in the source volume calculation below. Mean tidal range is the difference between MHW and MLW; this is the average excursion of the tide every 12.42 hrs. Diurnal range is the difference between MHHW and MLLW; this is the average difference between the highest and lowest tides of a tidal day

(24.84 hrs). Thus, it represents the average daily vertical excursion of the tide. The increase in tidal ranges in South Bay is evident. As confirmed by the semidiurnal/diurnal ratio $[(|M_2|+|S_2|+|N_2|)/ (|K_1|+|O_1|+ |P_1|)]$ in **Table 11**, the increase in range is due to the growth of the semidiurnal tide.

4.6.2 Estimation of the Source Volume V_S

The source volume V_S for larval entrainment calculations for the SBPP is defined as the volume of water below MWL and landward of the Coronado Narrows (**Figure 14**). There are two basic steps to computation of the source volume V_S. The first is compilation (using GIS software) of areas and volume below fixed elevations; for elevations above MLLW water, this was carried our at 1 ft intervals. It was then necessary to interpolate to determine areas and volumes below the tidal datum levels described in Section 4.6.1. The increase in tidal range in South Bay requires that South Bay be divided into a finite number of subdivisions, with tidal datum levels determined for each, either directly from a tide gauge in the subdivision or by interpolation from adjacent gauges. As a practical matter, the four subregions shown in **Figure 14** were employed. Tide gauges were available in subregions 2 to 4, whereas datum levels in subregion 1 had to be determined by interpolation. The manipulations of the tidal data needed to extract tidal datum levels have been described above. Accurate bathymetric data are also needed.

Bathymetry for subregions 1 and 2 and the periphery of regions 3 and 4 (west) came from the US Navy (US Navy, 1994). Bathymetry data collected Merkel and Associates were used for most of subregions 3 and 4. These data were collected using a Furuno FCV-600L single-beam fathometer operating at a frequency of 200 kHz. The echosounder was mounted on the port side of the vessel, with the 15º beam-width transducer located approximately half a foot below the water surface. Tidal elevation corrections were made using a gauge located on the Navy Pier. About 218 hectares adjacent to the discharge of the SBPP was surveyed by Tenera Environmental. A bathymetric survey provided bottom depths of the discharge area with centimeter horizontal and vertical accuracy using a BioSonics 200 kHz digital echosounder (8º beam-width transducer) with survey-quality base and roving GPS units. The base GPS was positioned on a Port Authority benchmark for referencing soundings to MLLW.

The resulting V_S subregion areas and volumes are tabulated in **Table 12**.

5.0 SUMMARY

The purpose of this report is to provide an oceanographic basis for definition of a source volume V_S for larval entrainment calculations applicable to the SBPP, San Diego Bay, California. Results are based both on interpretation of previous studies and on new analysis of tidal height and current data.

San Diego Bay is a Mediterranean, seasonally hypersaline estuary with a length of about 24.5 km from its ocean entrance to the head of South Bay. Most rainfall and river inflow occurs during the winter months, November to March. As a typical Mediterranean estuary, San Diego

Bay exhibits a marine zone near the mouth that is strongly influenced by the coastal ocean; a thermal zone (in north bay, the Narrows and the outer part of South Bay) that has weak thermally induced stratification and horizontal density gradients; and a hypersaline zone in which density increases toward the head of the bay. A riverine zone, present at the head of some Mediterranean estuaries, is absent or transient. South Bay, the primary zone of interest in this study, has weak circulation and a typical residence time R_T of weeks to about a month. Because mean flows are weak here and throughout most of the bay, exchange of water, salt, particles and organisms is controlled by tidal and possibly wind-driven dispersion, except perhaps for a few days after winter storms, when strong river outflow may occur.

This report has focused on the oceanographic background relevant to generalized calculations for organisms with a planktonic larval duration or PLD longer than a week. For these time scales, and for a longitudinal diffusivity K_H of ~20 m^2/s or greater, one can expect larvae to be mixed readily over distances comparable with the size of South Bay. With the possibility of enhanced mixing due to wind forcing and/or the influence of larval behavior, this suggests use of the well-defined South Bay (up to the Coronado Narrows) as the source volume for all populations with PLD of the order of a week to a month. This approach is consistent with estimates of residence time for South Bay, and the expectation that the internal mixing time of South Bay is between a week and a month. For longer PLD, the flux of larvae through the narrows should be taken into account and the source volume becomes more difficult to define. For shorter PLD, the source volume is smaller and more local to the vicinity of power plant—and the detail of flow patterns becomes important. This special case goes beyond the source volume approach to assessing the impact of larval entrainment.

Analysis of data from eight tide gauges suggests that there is a moderate increase in tidal amplitude and tidal range in the more landward parts of San Diego Bay. This amplification (primarily of the twice-daily or semidiurnal wave) is consistent with the idea that tides in San Diego Bay form a standing wave, though decreasing channel cross-sections in the more landward part of the system may cause some of the observed increase in tidal amplitudes in South Bay. There is also little generation of non-linear overtides through friction or wave distortion, probably because shallow tidal flats and marshes do not cover a large fraction of the bay. It is also likely that human alterations of depths, channel cross-sections and shorelines has somewhat altered the tides of San Diego Bay.

Analyses of mean and tidal currents measured at 18 locations throughout the interior of San Diego Bay show that tidal currents exhibit a local maximum in the Coronado Narrows and increase toward the bay mouth. Tidal currents are weak in South Bay and mean flows are weak throughout the bay, except at isolated locations. Estimates of tidal dispersion were also formed using data from the same 18 current meters. While spatial patterns are generally similar to those from Largier (1995), there are differences in detail. The measurements presented here provide superior temporal coverage to earlier studies, but some of the mechanisms (e.g., tidal pumping) found to be important at and seaward of the Narrows could not be calculated here. An important feature depicted both in our results and those of Largier is, however, that tidal dispersion has a local maximum at the Coronado Narrows, consistent with the idea that the Narrows acts as the "mouth" of South Bay. Overall, our results suggest that larvae are likely removed from South Bay primarily but not exclusively by dispersion. This idea is subject to the qualification that

advection may be dominant over tidal dispersion during winter river-flow events. Such events have not to date been measured.

These analyses of current patterns and tidal dispersion also justify the definition of a South Bay (south of the Coronado Narrows) as an appropriate source volume. These analyses confirm in a quantitative manner earlier definitions of eco-regions in San Diego Bay (e.g., Merkel and Associates 2000). In effect, the Coronado Narrows may be considered to be the "mouth" of South Bay. The Narrows is, therefore, a logical seaward boundary for the SBPP source volume.

V_S for the SBPP is defined as the volume below Mean Water Level (MWL, the average of a large number of tidal observations) in South Bay, south of the Coronado Narrows. In order to accurately determine the source volume V_S, volumes and areas below fixed elevations and standard tidal datum levels were tabulated for four subregions within V_S, based on tidal analysis results and bathymetric data.

6.0 REFERENCES

Bowden, K. F. 1983. Physical Oceanography of Coastal Waters. Ellis Horwood, London, pp. 259-279.

Chadwick, B., C. Katz, and J. Largier. 1995. Contaminant transport measurements in San Diego Bay. In: Proceedings Oceans '95.

Chadwick, D. B. and J. L. Largier. 1999a. The influence of tidal range on the exchange between San Diego Bay and the ocean. J Geophys Res 104, 29885-29900.

Chadwick, D. B. and J. L. Largier. 1999b. Tidal exchange at the bay-ocean boundary. J Geophys Res 104, 29901-29919.

Gutierrez de Velasco, G. and C. D. Winant. 2004. Wind and density-driven circulation in a well-mixed inverse estuary. J Phys Oceanogr 34 (in press)

DiBacco C., D. Sutton, and L. McConnico. 2001. Vertical migration behavior and horizontal distribution of brachyuran larvae in a low inflow estuary: Implications for bay-ocean exchange. Mar Ecol Prog Ser 217, 191-206.

Engineering Science. 1988. Tijuana Oceanographic Engineering Study.

Fischer, H. B., E. J. List, R. C. Y. Koh, J. Imberger, and N. H. Brooks. 1979. Mixing in Inland and Coastal Waters. Academic Press, San Diego. pp. 94-103 and 234-237.

Foreman, M. G. G., 1977. Manual for tidal heights analysis and prediction. IOS, Sidney, B.C.

Foreman, M. G. G., 1978. Manual for tidal currents analysis and prediction. IOS, Sidney, B.C.

George, R. A. and J. L. Largier. 1996. Lagrangian Drifter Observations in San Diego Bay: Data Report. Scripps Institution of Oceanography Reference Report.

Godin, G. 1972. The Analysis of Tides. University of Toronto Press, 264 pp., Toronto.

Intersea Research Corporation (IRC). 1980. Descriptive Physical Oceanography 316 (b) Study Final Report. La Jolla, CA., 69 pp., Appendices.

Largier, J. L. 1995. A study of the circulation of water in San Diego Bay for the purpose of assessing and monitoring and managing the transport and potential accumulation of pollutants and sediment in San Diego Bay. Final Report. Prepared for the California State Waters Resources Control Board. Scripps Institution of Oceanography, 31 pp, 6 Appendices.

Largier, J. L. 2001. Review of estimates of proportional loss of larvae from Morro Bay Estuary by entrainment into Morro Bay Power Plant cooling system Second Report. Regional Water Quality Control Board, Central Coast Region. Scripps Institute of Oceanography, 8 pp.

Largier, J. L., C. J. Hearn, and D. B. Chadwick, 1996. Density structures in low-inflow "estuaries". In: Buoyancy Effects on Coastal and Estuarine Dynamics. D. G. Aubrey and C. T. Friederichs (Eds.). Coastal and Estuarine Studies, 53, 227-241.

Largier, J. L., S. V. Smith, and J. T. Hollibaugh. 1997. Seasonally hypersaline estuaries in Mediterranean-climate regions. Estuar. Coast. Shelf Sci, 45, 789-797.

Lenz, C., 1976. A Compendium of Important Physical Factors for San Diego Bay. Unpublished Report.

Merkel and Associates, Inc. 2000. Environmental Controls on the Distribution of Eelgrass (*Zostera marina* L.) in South San Diego Bay. Merkel and Associates, Inc, San Diego, 81 pp. plus Appendices

Pawlowicz, R., B. Beardsley, and S. Lentz. 2002. Classical tidal harmonic analysis including error estimates in MATLAB using T_TIDE, Computers and Geosciences 28, 929-937

Peeling, T. J. 1974. A Proximate Biological Survey of San Diego Bay, California. Report No TP389.

Pringle J. M. and K. Riser. 2003. Remotely forced nearshore upwelling in southern California. J Geophys Res 108, 3131-3141,

Roughan, M., J. L. Largier, L. Clarke, and M. L. Carter, in prep. Estuarine dispersion and flushing time scales during stratified and non-stratified conditions. The case of Mission Bay, California, USA. To be submitted to Estuarine Coastal and Shelf Science.

Schiff, K., S. Bay, and D. Diehl, 2001. Stormwater Toxicity in Chollas Creek and San Diego Bay. SCCWRP Technical Report 340.

U.S. Coast and Geodetic Survey, 1952, Manual of Harmonic Constant Reduction, US Government Printing Office, Washington, DC, 72 pp.

U.S. Navy 1994. Bathymetric and Eelgrass Survey of San Diego Bay, California 1993. Southwest Division Natural Resources Branch.

Wang, P. F., R. T. Chang, K. Richter, E. S. Gross, D. Sutton, and J. W. Gartner. 1998. Modeling tidal hydrodynamics of San Diego Bay, California, J Am Water Res Assoc 34, 1123-1140.

Table 1. Tide stations, positions, deployment, and durations.

Tide Gauge Location	Station Symbol	Deployment Date	Duration Days	Latitude			Longitude		
				degr	min	sec	degr	min	sec
San Diego	TG0	1/1/1983	365.0	32	42	48	117	10	24
San Diego	TG0	1/1/1993	1095.0	32	42	48	117	10	24
Sweetwater	TG1	11/16/2003	43.9	32	38	54	117	6	48
South Bay	SB	9/16/1993	356.0	32	36	54	117	5	52
OS200	OS200	6/22/1993	63.9	32	40	26	117	13	31
Broadway	TG2	8/1/1983	61.0	32	42	48	117	10	24
Broadway	TG2	1/1/1990	365.0	32	42	48	117	10	24
Navy Pier	TG3	8/16/1983	43.8	32	42	42	117	11	12
Coast Guard	TG4	8/15/1983	45.0	32	43	30	117	10	54
Ballast Point	TG5	8/15/1983	44.9	32	41	11	117	14	0
Ballast Point	TG5	8/31/1993	42.8	32	41	11	117	14	0

Table 2. Current Meter Data.

Current Meter	Station	Depth m, MLLW	Deployment date	Record Length, days	Current Meter Type	Latitude			Longitude		
						degr	min	sec	degr	min	sec
Buoy41ms	A41	mid	6/16/1993	14.6	Endeco	32	38	30	117	7	25
Sta1	N1	4.3	9/7/1983	20.9	Aanderaa	32	38	42	117	7	22
Sta2	N2	10.1	9/9/1983	18.9	Aanderaa	32	39	44	117	7	32
Sta5	N4	2.1	8/22/1983	33.4	Aanderaa	32	40	29	117	8	58
Buoy28bs	A28	bottom	7/6/1993	33.7	Endeco	32	40	40	117	7	50
Buoy28ms	A28	mid	6/16/1993	28.1	Endeco	32	40	40	117	7	50
Sta6a	N5	4.3	8/22/1983	20.8	Aanderaa	32	40	58	117	8	34
Sta6b	N5	8.5	8/22/1983	15.4	Aanderaa	32	40	58	117	8	34
Buoy24bs	A24	bottom	6/16/1993	35.9	Endeco	32	36	35	117	7	50
Buoy24ms	A24	mid	7/7/1993	15.0	Endeco	32	36	35	117	7	50
ADCP	NB2	1 to 10	6/23/1993	64.7	ADCP	32	42	5	117	9	50
Sta9a	N8	4.3	9/9/1983	16.6	Aanderaa	32	41	53	117	9	50
Sta9b	N8	11.6	9/9/1983	17.9	Aanderaa	32	41	53	117	9	50
Sta10	N9	3.4	8/22/1983	20.8	Aanderaa	32	42	20	117	9	55
Sta11	N11	4.3	8/22/1983	18.3	Aanderaa	32	42	30	117	10	39
Sta12	N11	11.3	8/19/1983	23.9	Aanderaa	32	42	30	117	10	39
Sta15	N13	10.1	9/19/1983	19.6	Aanderaa	32	43	1	117	10	35
Sta17	N14	8.5	8/20/1983	22.9	Aanderaa	32	43	19	117	10	40
Sta18	N14	4.3	8/19/1983	22.5	Aanderaa	32	43	19	117	10	40
Sta13	N10	4.3	9/6/1983	20.1	Aanderaa	32	42	47	117	12	46
Sta14	N10	10.4	9/7/1993	18.6	Aanderaa	32	42	47	117	12	46
Sta16	N12	4.6	8/18/1983	18.9	Aanderaa	32	43	9	117	11	30
Sta8a	N7	4.3	8/18/1983	38.8	Aanderaa	32	41	45	117	13	57
sta8b	N7	10.4	8/18/1983	38.8	Aanderaa	32	41	45	117	13	57
Sta7	N6	1.5	9/16/1983	20.0	Aanderaa	32	41	4	117	13	56
Sta3a	N3	4.6	8/18/1983	38.9	Aanderaa	32	39	57	117	13	34
Sta3b	N3	10.1	8/18/1983	38.9	Aanderaa	32	39	57	117	13	34

Table 3. K_1 Tidal Characteristics.

Tide Gauge	Station Symbol	Deployment Date	Record Length, days	Amplitude m	Phase deg, κ
Ballast Point	TG5	8/15/1983	44.9	0.335	88
Ballast Point	TG5	8/31/1993	42.7	0.325	88
Coast Guard	TG4	8/15/1983	45.0	0.325	87
Broadway	TG2	8/1/1983	61.0	0.340	88
San Diego	TG0	9/16/1993	365.0	0.339	88
Navy Pier	TG3	8/16/1983	43.8	0.328	88
OS200	OS200	6/22/1993	63.9	0.345	90
Sweetwater	TG1	11/16/2003	43.9	0.334	89
South Bay	SB	9/16/1993	356.3	0.341	88

Table 4. M_2 Tidal Characteristics.

Tide Gauge	Station Symbol	Deployment Date	Record Length, days	Amplitude m	Phase deg, κ
Ballast Point	TG5	8/15/1983	44.9	0.506	270
Ballast Point	TG5	8/31/1993	42.7	0.520	271
Coast Guard	TG4	8/15/1983	45.0	0.518	271
Broadway	TG2	8/1/1983	61.0	0.535	273
San Diego	TGO	9/16/1993	365.0	0.548	272
Navy Pier	TG3	8/16/1983	43.8	0.526	272
OS200	OS200	6/22/1993	63.9	0.535	277
Sweetwater	TGI	11/16/2003	43.9	0.543	273
South Bay	SB	9/16/1993	356.3	0.572	271

Table 5. M_4 Tidal Characteristics.

Tide Gauge	Station Symbol	Deployment Date	Record Length, days	Amplitude m	Phase deg, κ
Ballast Point	TG5	8/15/1983	44.9	0.0052	165
Ballast Point	TG5	8/31/1993	42.8	0.0044	169
Coast Guard	TG4	8/15/1983	45.0	0.0015	111
Broadway	TG2	8/1/1983	61.0	0.0031	147
San Diego	TG0	9/16/1993	365.0	0.0036	161
Navy Pier	TG3	8/16/1983	43.8	0.0041	145
OS200	OS200	6/22/1993	63.9	0.0046	209
Sweetwater	TG1	11/16/2003	43.9	0.0021	116
South Bay	SB	9/16/1993	356.3	0.0050	100

Table 6. K_1 Tidal Current Characteristics.

Current Meter	Station Symbol	Depth	Deployment Date	Record Length, days	Major Axis Amp, cm/s	Minor Axis Amp, cm/s	Axis Direction, deg	Phase deg, κ
Buoy41ms	A41	mid	6/16/1993	14.6	1.35	-0.10	281	10
Sta1	N1	4.3	9/7/1983	20.9	4.68	0.83	280	4
Sta2	N2	10.1	9/9/1983	18.9	4.28	1.20	89	196
Sta5	N4	2.1	8/22/1983	33.4	1.83	1.28	54	219
Buoy28bs	A28	2	7/6/1993	33.7	3.22	-0.02	312	0
Buoy28ms	A28	mid	6/16/1993	28.1	2.50	0.31	308	0
Sta6a	N5	4.3	8/22/1983	20.9	6.07	0.79	316	348
Sta6b	N5	8.5	8/22/1983	15.5	5.60	0.38	302	340
Buoy24bs	A24	bottom	6/16/1993	36.0	4.64	0.30	317	342
Buoy24ms	A24	mid	7/7/1993	15.0	8.55	-0.45	315	353
nb2bin9	NB2	2	6/23/1993	64.7	10.94	-0.06	315	177
nb2bin2	NB2	9	6/23/1993	64.7	4.64	-0.07	324	170
Sta9a	N8	4.3	9/9/1983	16.6	9.73	0.30	317	1
Sta9b	N8	11.6	9/9/1983	17.9	6.97	0.39	318	349
Sta10	N9	3.4	8/22/1983	20.8	0.86	-0.09	55	339
Sta11	N11	4.3	8/22/1983	18.3	9.14	0.14	318	2
Sta12	N11	11.3	8/19/1983	23.9	5.61	0.13	322	3
Sta16	N12	4.6	8/18/1983	18.9	6.39	0.29	341	28
Sta15	N13	10.1	8/19/1983	19.6	1.00	0.02	69	116
Sta18	N14	8.5	8/20/1983	22.9	1.82	-0.03	326	246
Sta17	N14	4.3	8/19/1983	22.5	3.00	0.23	319	252
Sta13	N10	4.3	9/6/1983	20.1	7.98	-0.54	25	355
Sta14	N10	10.4	9/7/1983	18.6	5.16	0.37	23	351
Sta8a	N7	4.3	8/18/1983	38.8	6.24	-0.75	360	8
Sta8b	N7	10.4	8/18/1983	38.9	6.71	0.34	286	191
Sta7	N6	1.5	9/6/1993	20.0	5.43	1.31	31	335
Sta3a	N3	4.6	8/18/1983	38.9	9.7	2.76	295	183
Sta3b	N3	10.1	8/18/1983	38.9	5.78	2.09	285	188

Table 7. M_2 Tidal Current Characteristics.

Current Meter	Station Symbol	Depth	Deployment Date	Record Length, days	Major Axis Amp, cm/s	Minor Axis Amp, cm/s	Axis Direction, deg	Phase deg, κ
Buoy41ms	A41	mid	6/16/1993	14.6	3.07	-0.19	274	195
Sta1	N1	4.3	9/7/1983	20.9	10.67	-0.90	272	204
Sta2	N2	10.1	9/9/1983	18.9	10.41	-0.05	273	210
Sta5	N4	2.1	8/22/1983	33.4	10.46	0.76	275	172
Buoy28bs	A28	2	7/6/1993	33.7	7.67	-0.30	315	210
Buoy28ms	A28	mid	6/16/1993	28.1	7.80	-0.18	312	208
Sta6a	N5	4.3	8/22/1983	20.9	15.96	-0.96	316	198
Sta6b	N5	8.5	8/22/1983	15.5	11.76	-0.96	302	198
Buoy24bs	A24	bottom	6/16/1993	36.0	16.98	-0.87	319	187
Buoy24ms	A24	mid	7/7/1993	15.0	28.35	-1.77	317	186
nb2bin9	NB2	2	6/23/1993	64.7	33.84	0.30	315	5
nb2bin2	NB2	9	6/23/1993	64.7	13.97	-0.39	319	358
Sta9a	N8	4.3	9/9/1983	16.6	36.21	-1.96	316	184
Sta9b	N8	11.6	9/9/1983	17.9	27.17	-0.65	313	176
Sta10	N9	3.4	8/22/1983	20.8	3.65	0.75	56	214
Sta11	N11	4.3	8/22/1983	18.3	20.06	0.45	319	199
Sta12	N11	11.3	8/19/1983	23.9	13.84	0.11	325	194
Sta16	N12	4.6	8/18/1983	18.9	18.02	1.45	343	192
Sta15	N13	10.1	8/19/1983	19.6	4.16	-1.19	275	156
Sta18	N14	8.5	8/20/1983	22.9	2.10	-1.26	328	140
Sta17	N14	4.3	8/19/1983	22.5	4.22	0.04	317	125
Sta13	N10	4.3	9/6/1983	20.1	28.01	-0.45	27	184
Sta14	N10	10.4	9/7/1983	18.6	17.84	0.45	22	178
Sta8a	N7	4.3	8/18/1983	38.8	14.37	-0.25	271	24
Sta8b	N7	10.4	8/18/1983	38.9	20.50	-1.14	287	3
Sta7	N6	1.5	9/6/1993	20.0	19.73	1.57	38	171
Sta3a	N3	4.6	8/18/1983	38.9	30.00	0.91	286	14
Sta3b	N3	10.1	8/18/1983	38.9	18.65	3.09	294	4

Table 8. M_4 Tidal Current Characteristics.

Current Meter	Station Symbol	Depth	Deployment Date	Record Length, days	Major Axis Amp, cm/s	Minor Axis Amp, cm/s	Axis Direc-tion, deg	Phase deg, κ
Buoy41ms	A41	mid	6/16/1993	14.6	0.48	0.10	304	253
Sta1	N1	4.3	9/7/1983	20.9	2.15	-0.14	87	66
Sta2	N2	10.1	9/9/1983	18.9	0.34	-0.15	331	196
Sta5	N4	2.1	8/22/1983	33.4	0.63	-0.36	56	121
Buoy28bs	A28	2	7/6/1993	33.7	0.37	0.11	330	327
Buoy28ms	A28	mid	6/16/1993	28.1	0.36	0.02	296	334
Sta6a	N5	4.3	8/22/1983	20.9	0.64	0.07	24	109
Sta6b	N5	8.5	8/22/1983	15.5	0.36	0.00	67	303
Buoy24bs	A24	bottom	6/16/1993	36.0	1.15	0.05	15	52
Buoy24ms	A24	mid	7/7/1993	15.0	1.59	-0.58	338	16
nb2bin9	NB2	2	6/23/1993	64.7	1.13	-0.14	315	123
nb2bin2	NB2	9	6/23/1993	64.7	0.73	0.19	338	80
Sta9a	N8	4.3	9/9/1983	16.6	1.08	-0.81	291	330
Sta9b	N8	11.6	9/9/1983	17.9	1.23	-0.43	299	302
Sta10	N9	3.4	8/22/1983	20.8	0.40	0.13	89	41
Sta11	N11	4.3	8/22/1983	18.3	0.89	0.29	24	282
Sta12	N11	11.3	8/19/1983	23.9	1.82	0.13	333	317
Sta16	N12	4.6	8/18/1983	18.9	0.83	-0.04	8	46
Sta15	N13	10.1	8/19/1983	19.6	2.147	-0.331	279	354
Sta18	N14	8.5	8/20/1983	22.9	0.66	-0.06	299	84
Sta17	N14	4.3	8/19/1983	22.5	0.83	0.21	311	141
Sta13	N10	4.3	9/6/1983	20.1	1.16	-0.06	40	358
Sta14	N10	10.4	9/7/1983	18.6	0.80	-0.03	325	26
Sta8a	N7	4.3	8/18/1983	38.8	1.78	-0.40	288	302
Sta8b	N7	10.4	8/18/1983	38.9	0.61	0.22	53	320
Sta7	N6	1.5	9/6/1993	20	4.23	-0.43	71	23
Sta3a	N3	4.6	8/18/1983	38.9	3.19	0.50	88	267
Sta3b	N3	10.1	8/18/1983	38.9	2.46	0.68	293	80

Table 9. Mean Current Flows.

Current Meter	Station Symbol	Depth m	Deployment Date	Record length Days	Speed cm/s	Direction deg, k
Buoy41ms	A41	mid	6/16/1993	14.6	0.79	179
Sta1	N1	4.3	9/7/1983	20.9	4.21	129
Sta2	N2	10.1	9/9/1983	18.9	1.11	220
Sta5	N4	2.1	8/22/1983	33.4	0.96	161
Buoy28bs	A28	2	7/6/1993	33.7	0.48	132
Buoy28ms	A28	mid	6/16/1993	28.1	0.17	145
Sta6a	N5	4.3	8/22/1983	20.9	1.78	332
Sta6b	N5	8.5	8/22/1983	15.5	0.63	309
Buoy24bs	A24	bottom	6/16/1993	36.0	2.32	6
Buoy24ms	A24	mid	7/7/1993	15.0	1.97	24
nb2bin9	NB2	2	6/23/1993	64.7	2.30	313
nb2bin2	NB2	9	6/23/1993	64.7	0.95	12
Sta9a	N8	4.3	9/9/1983	16.6	1.74	64
Sta9b	N8	11.6	9/9/1983	17.9	1.42	39
Sta10	N9	3.4	8/22/1983	20.8	2.17	62
Sta11	N11	4.3	8/22/1983	18.3	3.04	193
Sta12	N11	11.3	8/19/1983	23.9	1.00	310
Sta16	N12	4.6	8/18/1983	18.9	3.13	132
Sta18	N14	8.5	8/20/1983	22.9	2.04	120.77
Sta17	N14	4.3	8/19/1983	22.5	2.80	358.44
Sta13	N10	4.3	9/6/1983	20.1	1.34	192
Sta14	N10	10.4	9/7/1983	18.6	1.54	326.29
Sta8a	N7	4.3	8/18/1983	38.8	2.88	200.32
Sta8b	N7	10.4	8/18/1983	38.9	5.59	83.73
Sta7	N6	1.5	9/6/1993	20	5.59	79.89
Sta3a	N3	4.6	8/18/1983	38.9	4.11	187.9
Sta3b	N3	10.1	8/18/1983	38.9	6.29	139.06

Table 10. Tidal Dispersion Characteristics.

Current Meter	Station	Depth/m	Deployment date	Duration days	RMS K_H (m2s-1)	Spring Tide K_H (m2s-1)	Neap Tide K_H (m2s-1)
Buoy41ms	A41	mid	6/16/1993	14.6	35.9	40	60
Sta1	N1	4.3	9/7/1983	20.9	37.9	50	70
Sta2	N2	10.1	9/9/1983	18.9	46.2	35	50
Sta5	N4	2.1	8/22/1983	33.4	7.4	5	10
Buoy28bs	A28	2	7/6/1993	33.7	31.7	35	45
Buoy28ms	A28	mid	6/16/1993	28.1	39.1	40	30
Sta6a	N5	4.3	8/22/1983	20.9	33.6	30	40
Sta6b	N5	8.5	8/22/1983	15.5	42.4	60	50
Buoy24bs	A24	bottom	6/16/1993	36	54.2	60	40
Buoy24ms	A24	mid	7/7/1993	15	35.9	60	30
nb2bin9	NB2	2	6/23/1993	64.7	88.7	150	50
nb2bin7	NB2	4	6/23/1993	64.7	86.7	135	50
nb2bin6	NB2	5	6/23/1993	64.7	81.5	130	50
nb2bin5	NB2	6	6/23/1993	64.7	77.1	120	50
nb2bin2	NB2	9	6/23/1993	64.7	51.4	80	40
nb2bin1	NB2	10	6/23/1993	64.7	55.5	100	40
Sta9a	N8	4.3	9/9/1983	16.6	54.0	60	40
Sta9b	N8	11.6	9/9/1983	17.9	32.2	30	40
Sta10	N9	3.4	8/22/1983	20.8	58.8	30	100
Sta11	N11	4.3	8/22/1983	18.3	43.2	40	55
Sta12	N11	11.3	8/19/1983	23.9	47.2	40	100
Sta15	N13	10.1	8/19/1983	19.6	43.9	60	50
Sta17	N14	8.5	8/19/1983	22.5	58.2	60	40
Sta18	N14	4.3	8/20/1983	22.9	49.0	60	35
Sta16	N12	4.6	8/18/1983	18.9	58.4	65	40
Sta13	N10	4.3	9/6/1983	20.1	46.2	60	20
Sta14	N10	10.4	9/7/1983	18.6	32.9	60	50
Sta8a	N7	4.3	8/18/1983	38.8	75.8	100	60
Sta8b	N7	10.4	8/18/1983	38.8	71.3	80	70
Sta7	N6	1.5	9/6/1983	20	69.1	60	80
Sta3a	N3	4.6	8/18/1983	38.9	79.1	80	120
Sta3b	N3	10.1	8/18/1983	38.9	54.1	80	40

RMS = root mean square

Table 11. Tidal Datum Levels and Tidal Properties for San Diego Bay. Abbreviations are defined in the text of this report.

Station:	**La Jolla**	**Ballast Pt**	**Coast Guard**	**Broadway**	**San Diego**	**Navy Wharf**	**OS200**	**Sweetwater**	**South Bay**
Symbol:		**TG5**	**TG4**	**TG2**	**TG0**	**TG3**	**OS200**	**TG1**	**SB**
Property:									
Position, km	-	2.29	8.3	9.38	9.63	9.02	15	19.3	22.38
EHW, m	2.332	-	-	-	2.481	-	-	-	-
MHHW, m	1.621	1.678	1.697	1.743	1.745	1.710	1.742	1.761	1.801
MHW, m	1.402	1.468	1.479	1.520	1.519	1.492	1.517	1.539	1.581
MLHW, m		1.257	1.261	1.277	1.293	1.274	1.292	1.317	1.360
MTL, m	0.839	0.870	0.881	0.905	0.902	0.887	0.905	0.914	0.933
MWL, m	0.833	0.861	0.876	0.898	0.896	0.880	0.896	0.910	0.929
MHLW, m		0.544	0.566	0.578	0.570	0.562	0.585	0.578	0.572
MLW, m	0.276	0.272	0.283	0.289	0.285	0.281	0.292	0.289	0.286
NAVD-88, m	0.058	-	-	-	0.132	-	-	-	-
MLLW, m	0	0.000	0.000	0.000	0.000	0.000	0.000	0.000	0.000
ELW, m	-0.874	-	-	-	-0.942	-	-	-	-
Diurnal Range	1.621	1.678	1.697	1.743	1.745	1.710	1.742	1.761	1.801
Mean Range	1.125	1.196	1.196	1.231	1.234	1.211	1.225	1.250	1.295
diurnal/	-	1.292	1.336	1.340	1.360	1.360	1.279*	1.374	1.414
semidurnal ratio									

* The semidiurnal/diurnal ratio is anomalously low at OS200 because the N2 amplitude is low; this may be a result of limited record length.

Table 12a. Region 1 Source Volume Areas and Volume, by Elevation and Sub-Area.

Datum	ht (MLLW)		2D Area Sq ft	2D Area Sq m	Volume Cu ft	Volume Cu m
	ft	m				
	6.00	1.829	45,785,641	4,253,210	1,333,028,542	37,741,679
MHHW	5.69	1.734	45,785,641	4,253,210	1,318,834,994	37,339,821
	5.00	1.524	45,785,641	4,253,210	1,287,242,901	36,445,362
MHW	4.96	1.513	45,785,641	4,253,210	1,285,548,832	36,397,398
	4.00	1.219	45,785,641	4,253,210	1,241,457,260	35,149,046
	3.00	0.914	45,785,641	4,253,210	1,195,288,288	33,841,876
MTL	2.95	0.9003	45,693,611	4,244,661	1,193,071,768	33,779,120
MWL	2.93	0.8976	45,656,798	4,241,241	1,192,185,160	33,754,018
	2.00	0.6096	43,945,028	4,082,228	1,150,957,891	32,586,761
	1.00	0.3048	43,700,500	4,059,513	1,106,961,518	31,341,104
MLW	0.89	2.931	43,679,534	4,057,565	1,102,284,715	31,208,691
MLLW	0.00	0.000	43,504,559	4,041,311	1,063,253,075	30,103,598
	-1.00	-0.3048	43,325,079	4,024,639	1,019,748,124	28,871,854
	-2.00	0.6096	43,153,454	4,008,696	976,460,962	27,646,277
	-5.00	-1.524	42,618,929	3,959,042	847,793,595	24,003,352
	-10.00	-3.048	34,720,557	3,225,330	654,886,339	18,541,621

Table 12b. Region 2 Source Volume Areas and Volume, by Elevation and Sub-Area.

Datum	ht (MLLW)		2D Area Sq ft	2D Area Sq m	Volume Cu ft	Volume Cu m
	ft	m				
	6.00	1.83	109,524,679	10,174,146	2,820,681,493	79,861,197
MHHW	5.73	1.75	109,524,679	10,174,146	2,790,602,730	79,009,585
	5.00	1.52	109,524,679	10,174,146	2,711,156,814	76,760,254
MHW	4.99	1.52	109,524,679	10,174,146	2,709,535,848	76,714,360
	4.00	1.22	109,524,679	10,174,146	2,601,632,134	73,659,311
	3.00	0.91	109,524,679	10,174,146	2,492,102,836	70,558,237
MTL	2.97	0.91	109,518,545	10,173,576	2,488,987,647	70,470,038
MWL	2.94	0.90	109,512,412	10,173,006	2,486,068,457	70,387,388
	2.00	0.61	109,320,223	10,155,153	2,382,605,847	67,458,079
	1.00	0.30	109,193,274	10,143,360	2,273,274,567	64,362,612
MLW	0.95	0.29	109,183,645	10,142,466	2,195,295,178	62,154,802
MLLW	0.00	0.00	109,000,706	10,125,472	2,164,105,606	61,271,740
	-1.00	-0.30	108,592,918	10,087,591	2,055,283,842	58,190,699
	-2.00	-0.61	107,998,207	10,032,346	1,946,946,723	55,123,379
	-5.00	-1.52	105,853,727	9,833,138	1,626,094,663	46,039,181
	-10.00	-3.05	100,942,483	9,376,914	1,107,178,869	31,347,258

Table 12c. Region 3 Source Volume Areas and Volume, by Elevation and Sub-Area.

Datum	ht (MLLW)		2D Area Sq ft	2D Area Sq m	Volume Cu ft	Volume Cu m
	ft	m				
	6.00	1.83	68,490,766	6,362,356	1,091,278,951	30,897,088
MHHW	5.78	1.76	68,490,766	6,362,356	1,076,135,643	30,468,339
MHW	5.04	1.54	68,490,766	6,362,356	1,025,308,645	29,029,288
	5.00	1.52	68,490,766	6,362,356	1,022,788,185	28,957,927
	4.00	1.22	68,490,766	6,362,356	954,297,419	27,018,766
	3.00	0.91	68,490,766	6,362,356	885,771,907	25,078,622
MTL	2.99	0.91	68,448,332	6,358,414	885,399,671	25,068,083
MWL	2.99	0.91	68,417,214	6,355,524	885,120,494	25,060,179
	2.00	0.61	61,418,380	5,705,377	823,732,561	23,322,119
	1.00	0.30	59,722,652	5,547,854	762,984,321	21,602,170
MLW	0.95	0.29	59,599,628	5,536,426	759,793,768	21,511,837
MLLW	0.00	0.00	57,461,169	5,337,777	704,356,005	19,942,242
	-1.00	-0.30	56,073,006	5,208,825	647,608,609	18,335,568
	-2.00	-0.61	54,768,951	5,087,687	592,106,151	16,764,142
	-3.00	-0.91	53,507,083	4,970,468	537,971,560	15,231,444
	-5.00	-1.52	50,241,902	4,667,153	434,008,441	12,287,964
	-10.00	-3.05	41,164,627	3,823,932	208,271,139	5,896,725

Table 12d. Region 4 Source Volume Areas and Volume, by Elevation and Sub-Area.

Datum	ht (MLLW)		2D Area Sq ft	2D Area Sq m	Volume Cu ft	Volume Cu m
	ft	m				
	6.00	1.83	103,278,651	9,593,929	1,030,375,861	29,172,755
MHHW	5.91	1.80	103,278,651	9,593,929	1,020,915,536	28,904,907
MHW	5.19	1.58	103,278,647	9,593,929	946,327,695	26,793,122
	5.00	1.52	103,278,651	9,593,929	927,097,210	26,248,654
	4.00	1.22	103,278,608	9,593,925	823,817,410	23,324,521
MTL	3.06	0.93	102,885,393	9,557,398	726,969,049	20,582,479
MWL	3.05	0.93	102,879,765	9,556,875	720,895,066	20,410,508
	3.00	0.91	102,859,479	9,554,991	720,586,267	20,401,765
	2.00	0.61	97,729,117	9,078,413	621,236,636	17,588,906
	1.00	0.30	92,861,251	8,626,219	525,641,158	14,882,337
MLW	0.94	0.29	92,434,175	8,586,547	520,052,796	14,724,115
MLLW	0.00	0.00	86,006,096	7,989,419	435,940,327	12,342,661
	-1.00	-0.30	74,068,630	6,880,504	355,538,747	10,066,273
	-2.00	-0.61	65,332,208	6,068,946	286,113,770	8,100,662
	-5.00	-1.52	34,855,985	3,237,899	134,856,101	3,818,145
	-10.00	-3.05	10,144,829	942,390	38,322,663	1,085,019

Figure 1a. An aerial view of San Diego Bay and environs from http://regionalworkbench.org/images/sdtj_nasa.jpg. Pt Loma is at center left. The SBPP is just northeast of the bright green salt pans at the south end of South Bay.

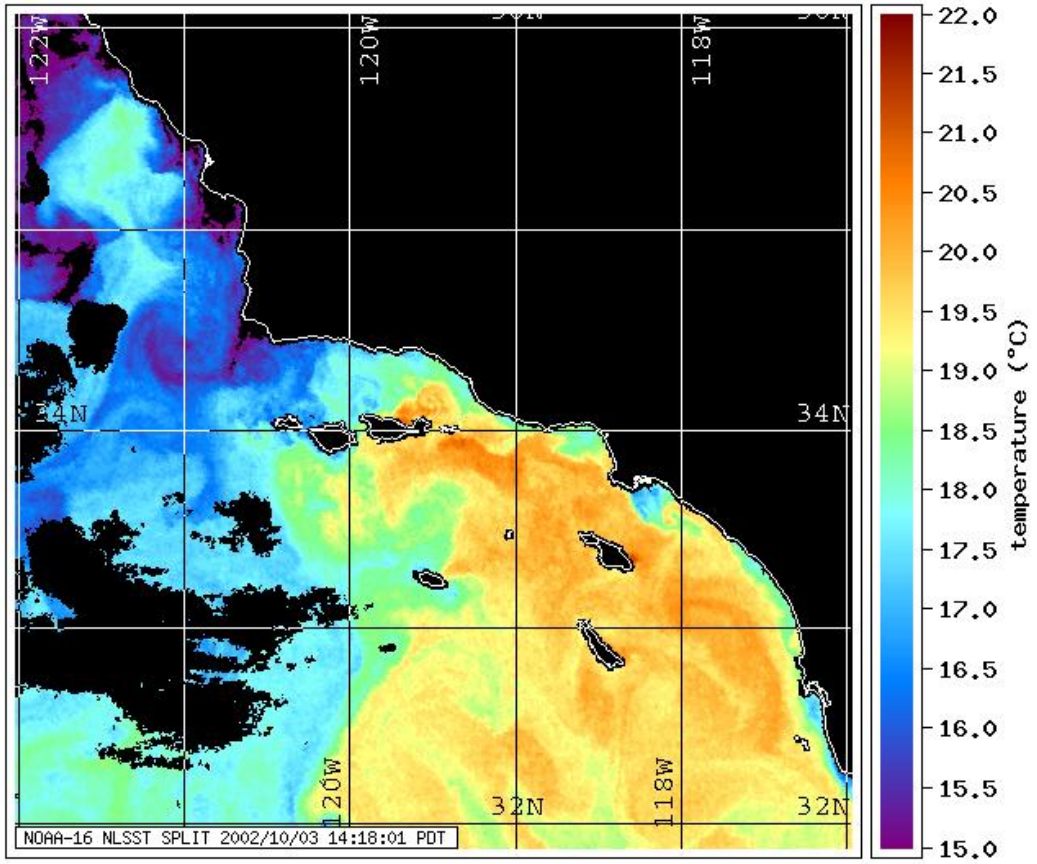

Figure 1b. A NOAA satellite AVHRR image of the temperature distribution off Southern California for 10/3/2002. Most of the waters in the Southern California Bight south of 34º 30' N are much warmer than coastal waters to the north of Pt Conception. Some cooler coastal waters, indicative of upwelling, are seen at lower right within the Coronado Bight, especially south of Pt Loma and at the mouth of San Diego Bay. The bay mouth is at 32º 40' N.

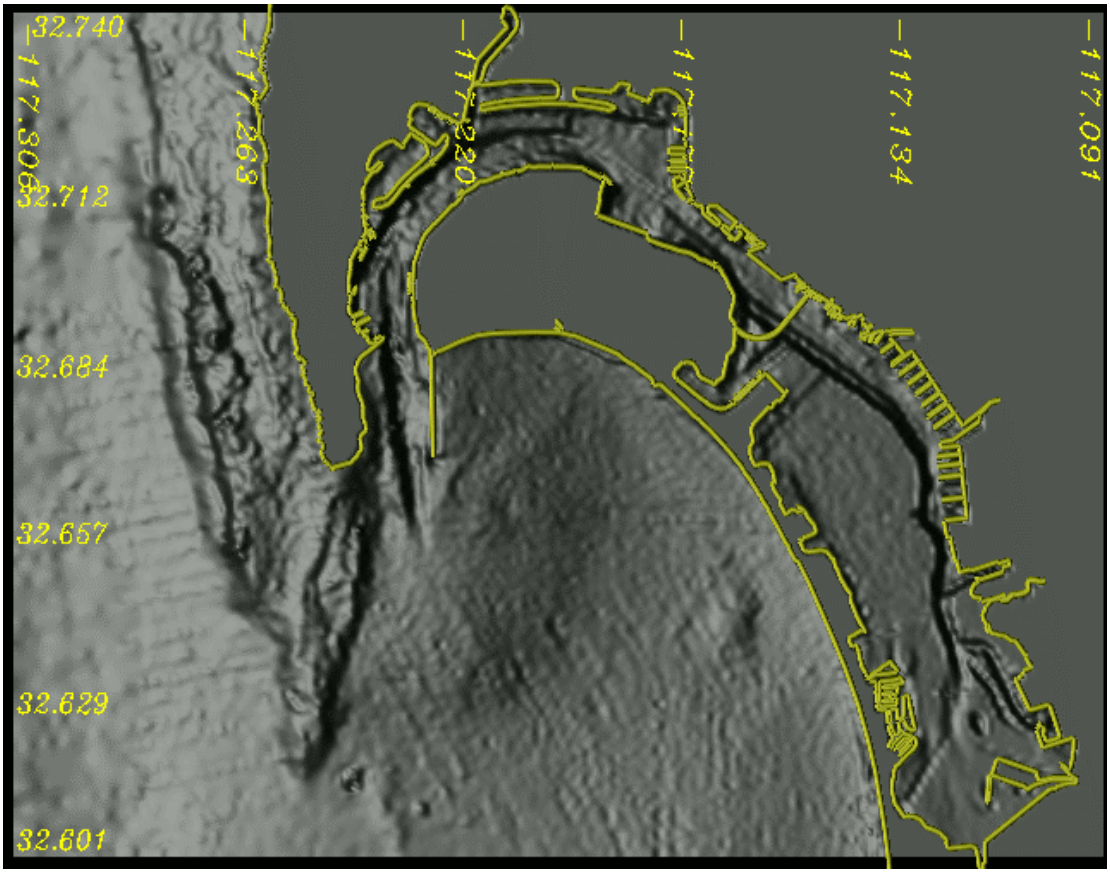

Figure 2. San Diego bay bathymetry; note the deep channels, from http://sdbay.sdsc.edu/html/modeling2.html.

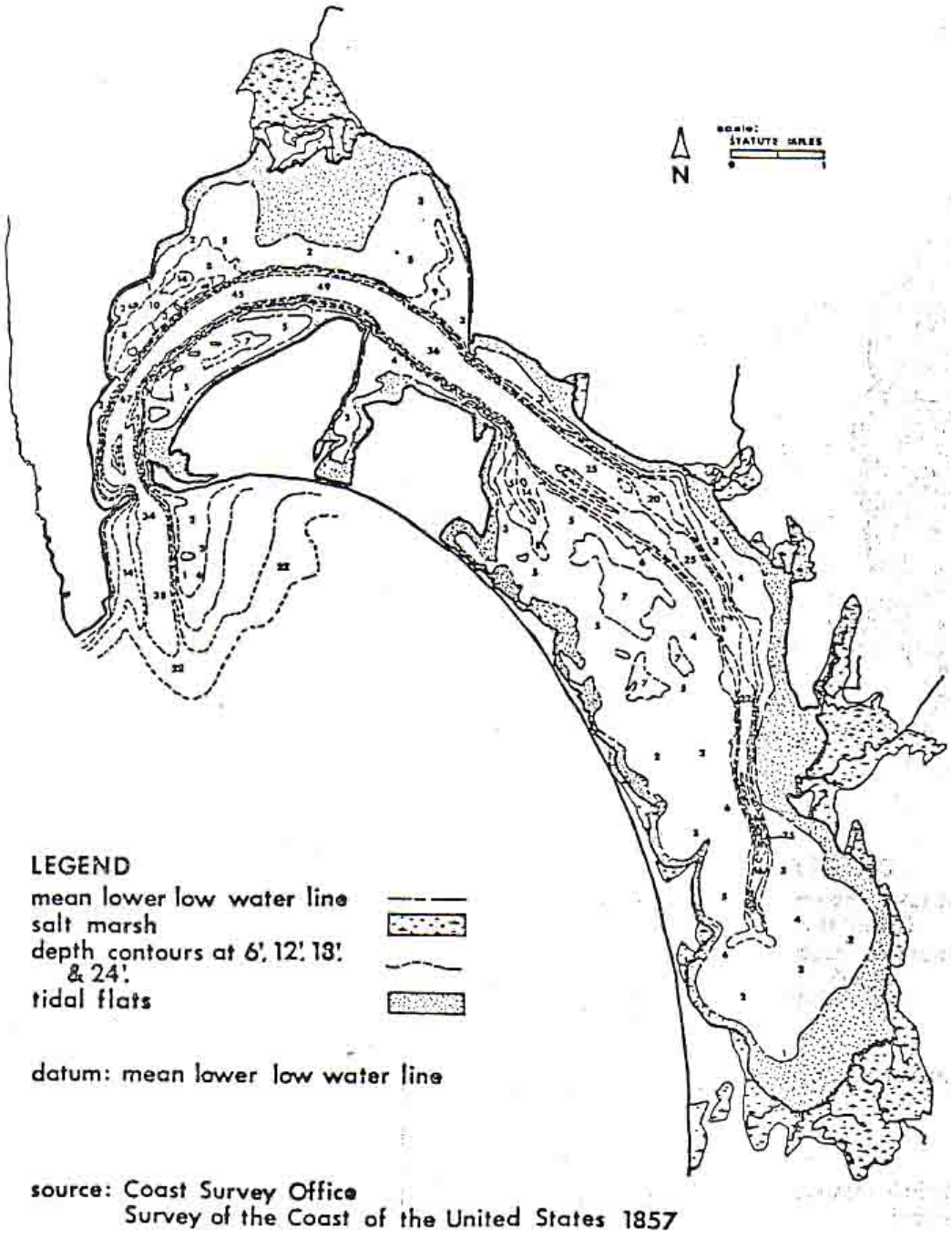

Figure 3. The 1857 configuration of San Diego Bay before most human alterations, compiled from US Coast and Geodetic survey sheets by IRC (1980). Note the narrow and unstable ocean spit and the changes in topography near the mouths of the Otay, Sweetwater and San Diego Rivers; the flow of the latter was diverted in 1852. The estuary has been shortened by the construction of salt pans near the Otay Rivers. While the present channel configuration is generally similar to the 1857, extensive dredging has deepened the bay, and most shorelines have been dredged and/or filled.

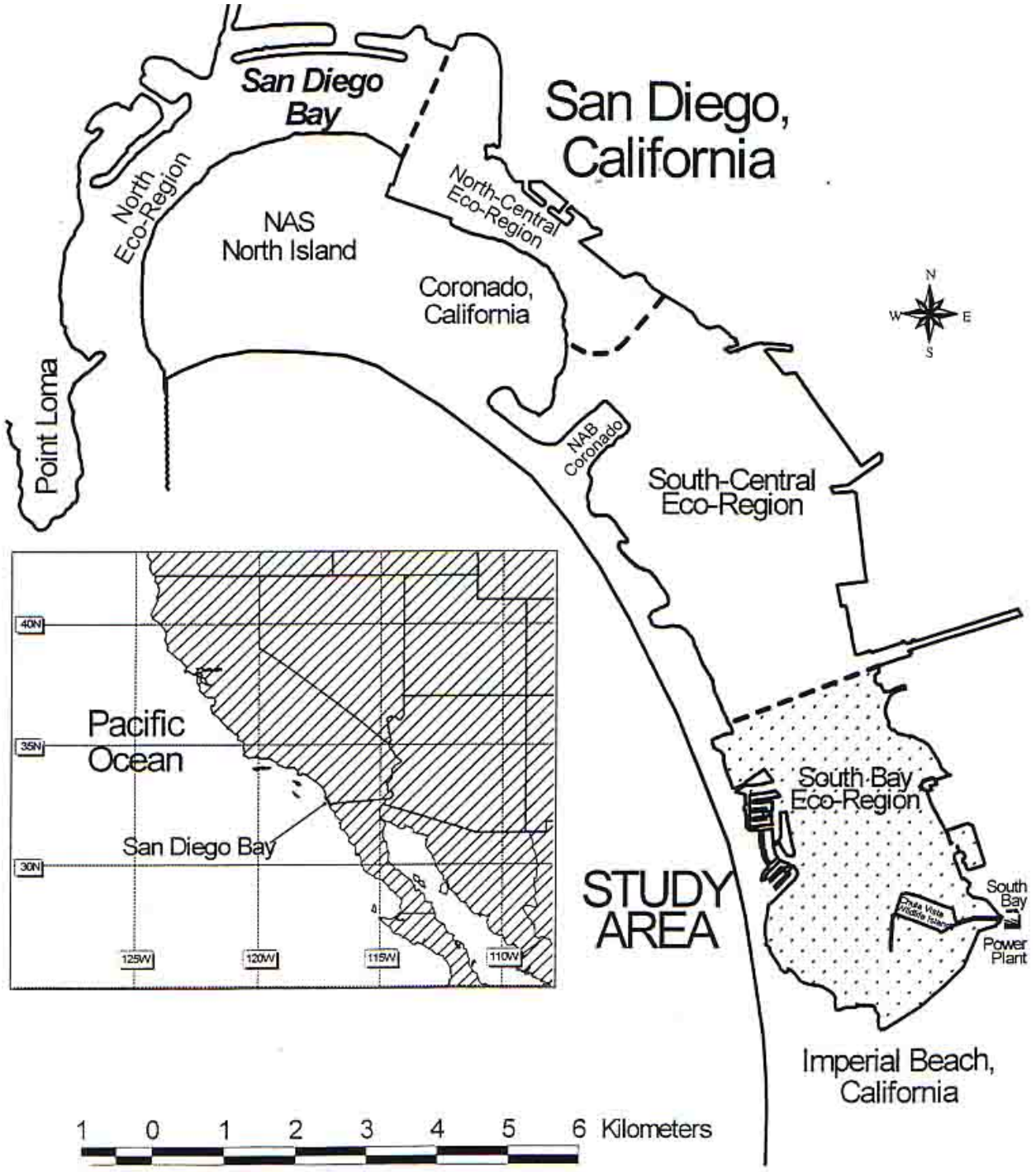

Figure 4. San Diego Bay eco-regions, from Merkel and Associates (2000). The SBPP is in the South Bay Eco-Region.

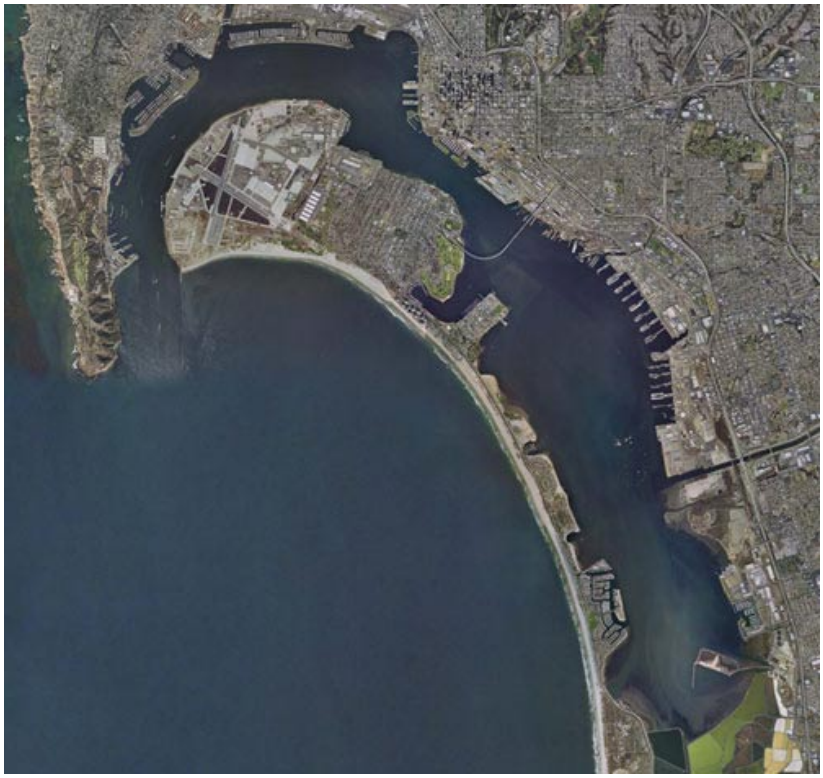

Figure 5. Overhead view of San Diego Bay from http://www.sdmis.org/view/bay-overview. phtml. Note the color-change in South Bay, which may indicate turbidity, and the salt pans adjacent to the south end of South Bay.

Figure 6. The San Diego Bay tributary watershed; from www.portofsandiego.org/ sandiego_ environment/storm_water.asp

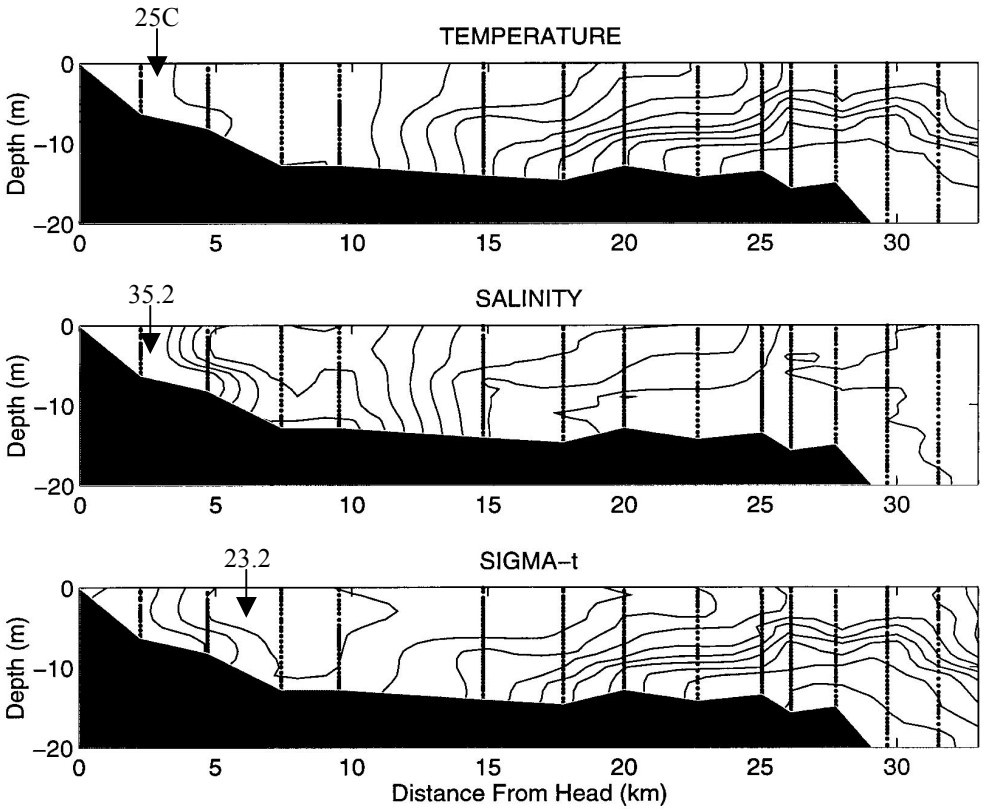

Figure 7. A vertical-longitudinal section of water temperature, salinity, and density (sigma-t) on 5 August 1993, representative of summer conditions in San Diego Bay. The mouth of the Bay (end of Zuniga jetty) is at 24.5 km. The narrows are about 13 km from the head of the Bay. Temperature contour interval is 1°C, with isotherms from 14 to 25°C. Salinity contour interval is 0.2, with isohalines from 33.2 to 35.2. Density (sigma-t) contour interval is 0.2, with isopycnals from 23.2 to 25.0; note the density minimum between 5 and 10 km from the head.

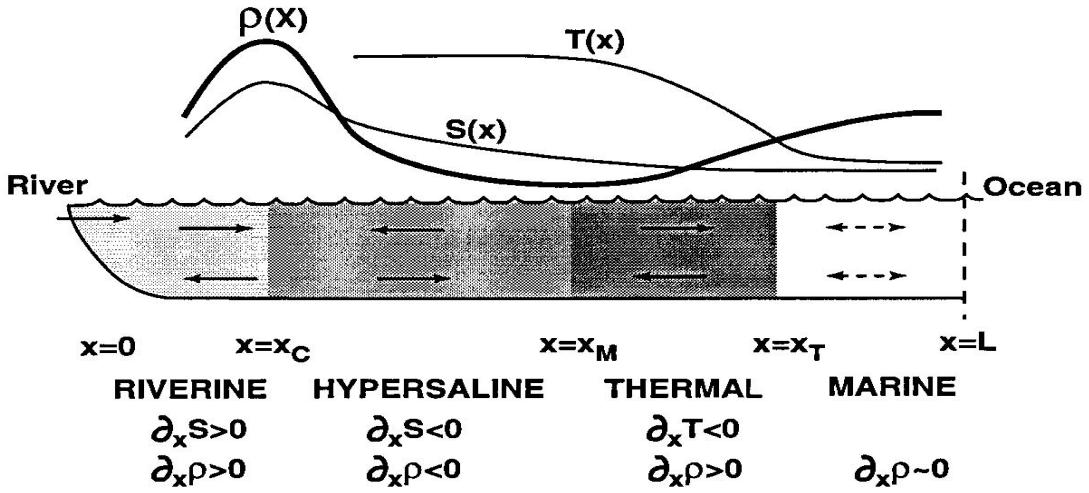

Figure 8. Schematic of longitudinal zones in a low-inflow estuary, like San Diego Bay (following Largier et al, 1996).

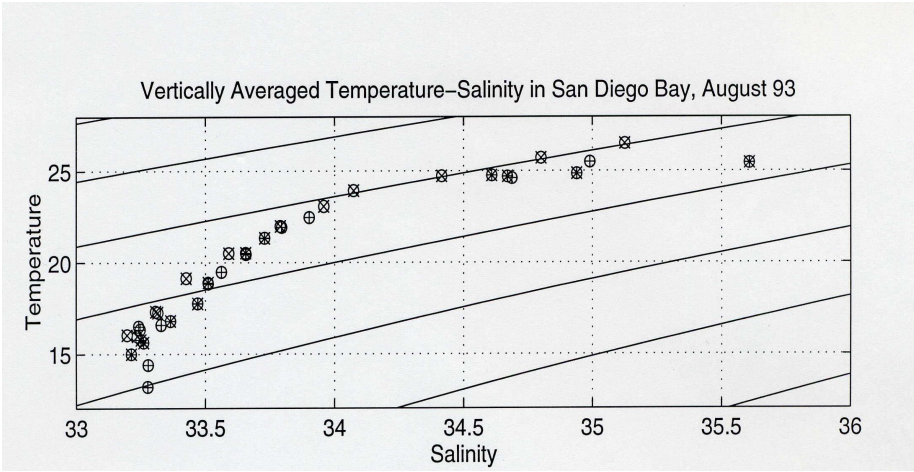

Figure 9. Temperature-salinity data from San Diego Bay, 5 August 1993 (cf., Figure 7), plotted over lines of equal density. Note the density minimum at a salinity of ~34.9 in mid-bay, between thermal zone of outer bay and hypersaline zone of the inner bay.

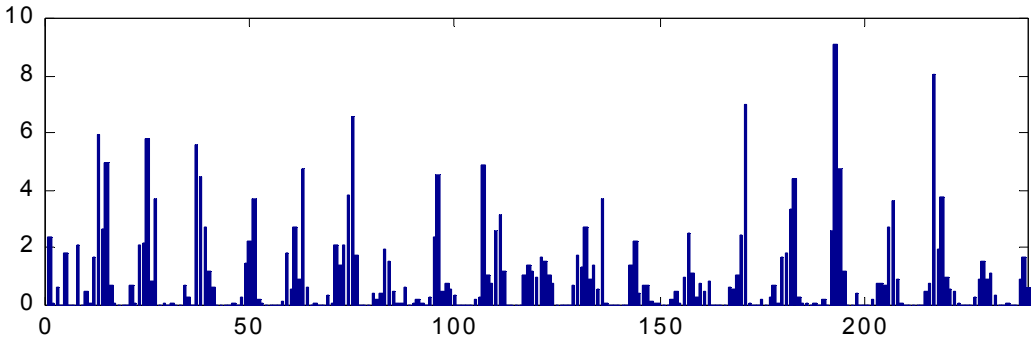

Figure 10. Monthly rain at Lindbergh Field airport, Jan 1977 to Dec 1996 – each monthly total is plotted as a bar (data in inches).

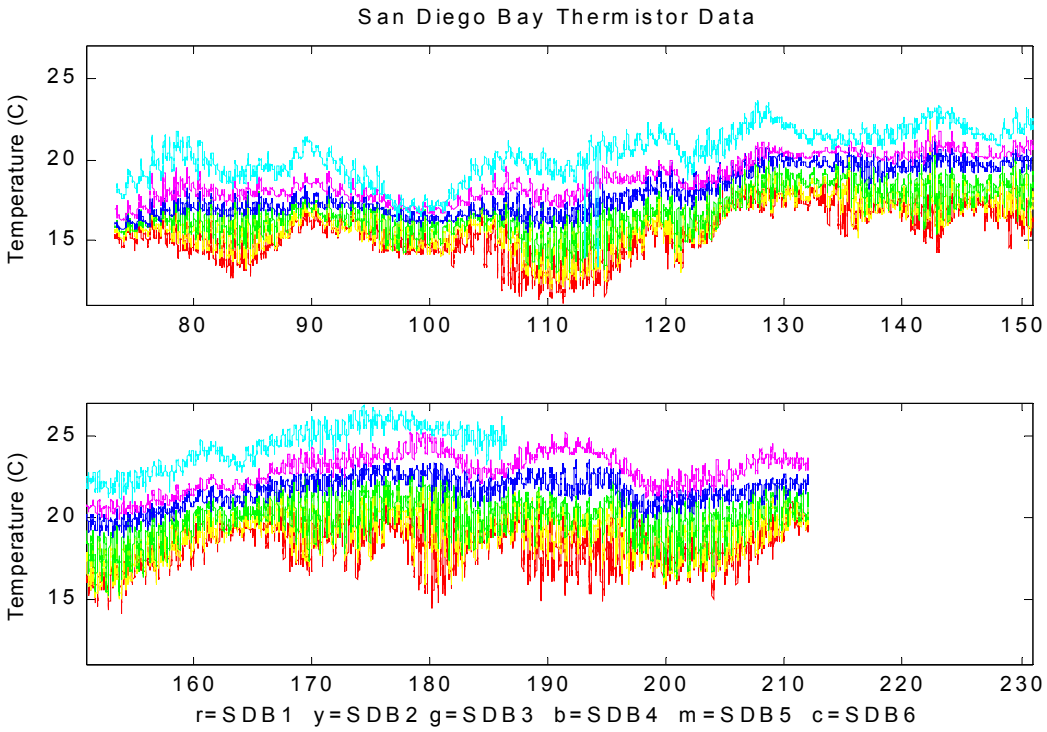

Figure 11. Surface water temperature in San Diego Bay 15 March to 31 July 2001 (time in Julian days). Data from channel markers 10 (red), 15 (yellow), 19 (green), 23 (blue), 30 (magenta), 41 (cyan). Marker #23 is in the narrows, with markers #30 and #41 in South Bay, off National City and Chula Vista; from unpublished data (Largier et al).

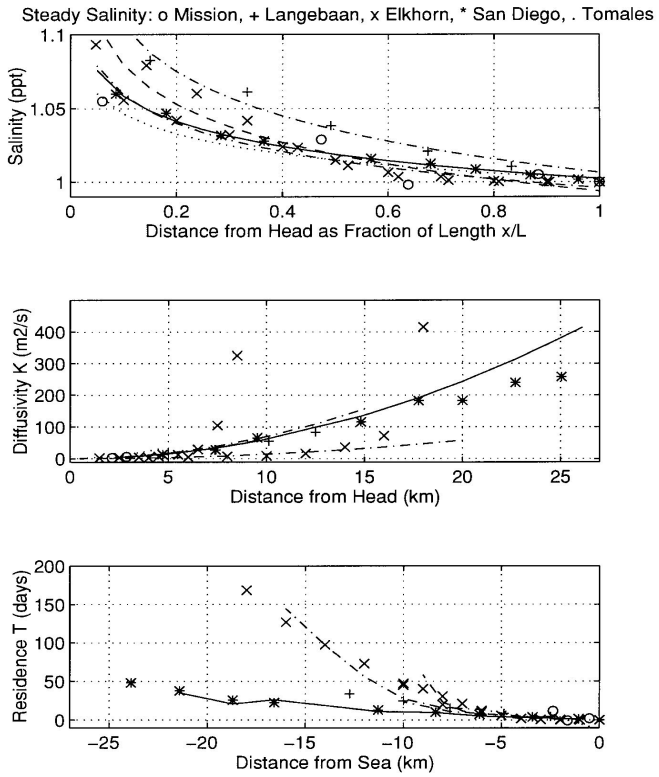

Figure 12a. Normalized salinity, estimated tidal diffusivity, and estimated residence times for San Diego Bay (indicated by ∗) and other seasonally hypersaline bays (from Largier et al, 1997).

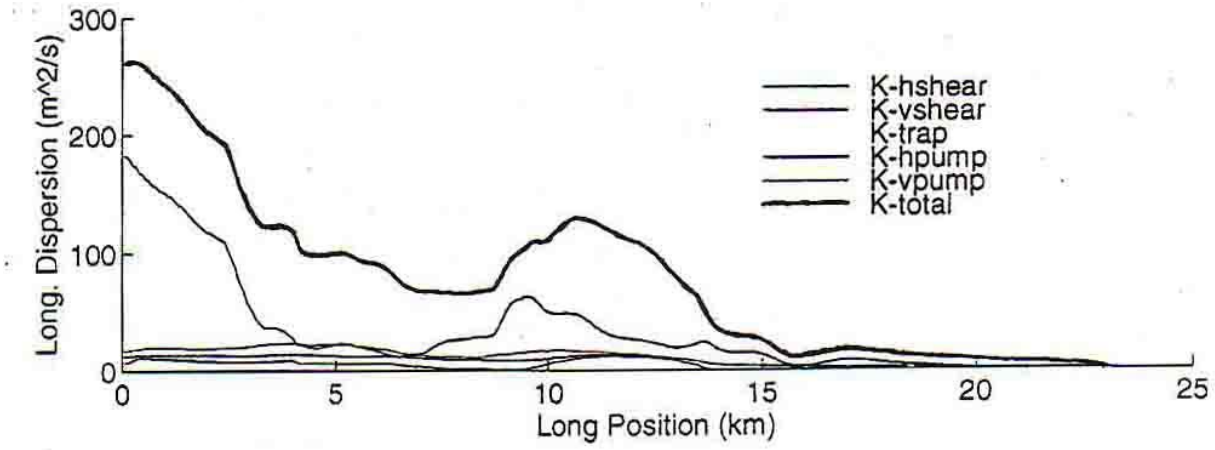

Figure 12b. Spatial distribution of selected longitudinal tidal dispersion mechanisms contributing to K_H (from Largier et al. 1995). There is a conspicuous maximum in total K_H at the Coronado Narrows. Tidal pumping processes are important from just seaward of the Narrows seaward, but are small in South Bay. The head of the bay is at ~km-24.5.

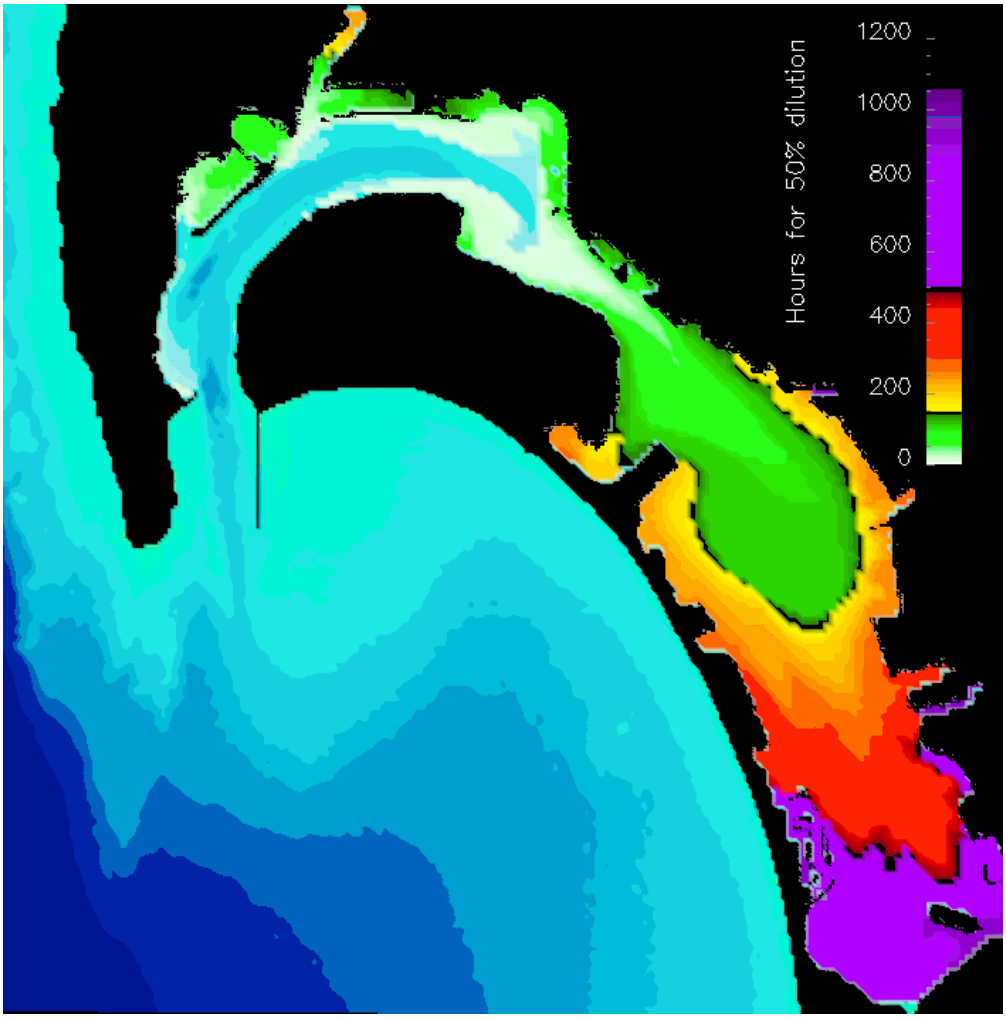

Figure 13. Numerical model estimates of the time required for exchange of 50% of a tracer uniformly mixed throughout the bay, assuming a tidal amplitude of 1m; from http://sdbay.sdsc.edu/html/modeling2.html. Even with above-average amplitude tides, 600–1000 hrs are required to exchange waters in South Bay.

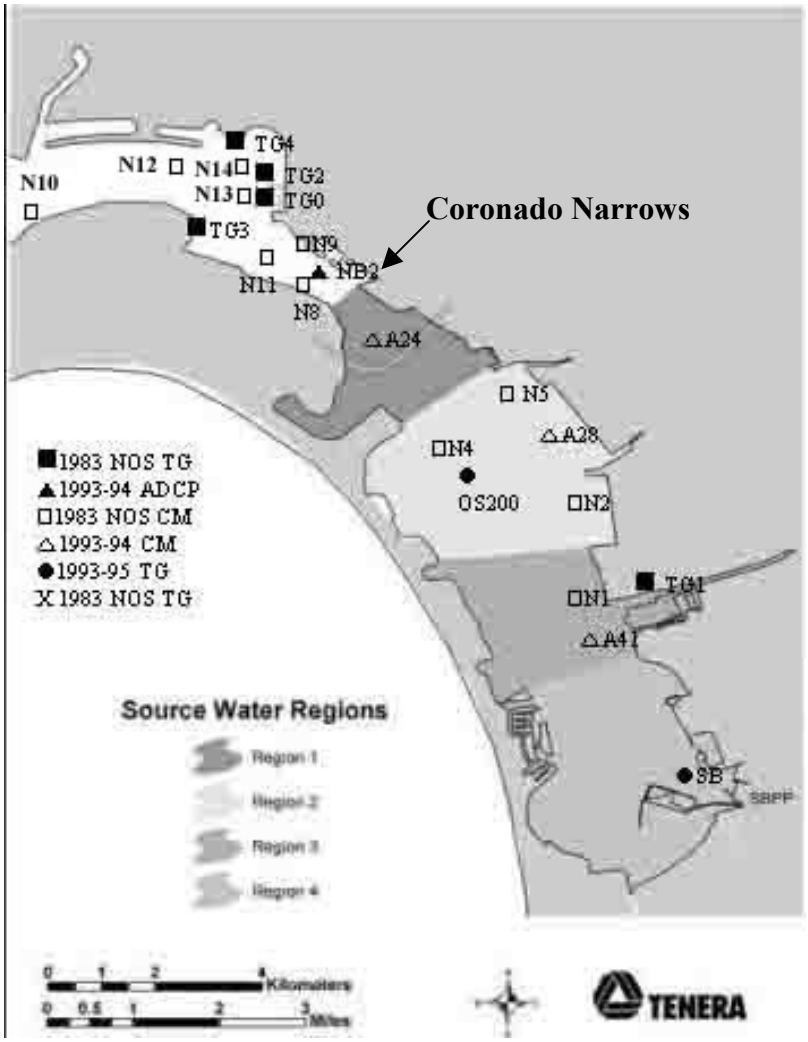

Figure 14. Station locations used in analyses of tidal elevations, tidal and mean currents and tidal dispersion. The four subregions used to compute the larval entrainment source volume are also shown.

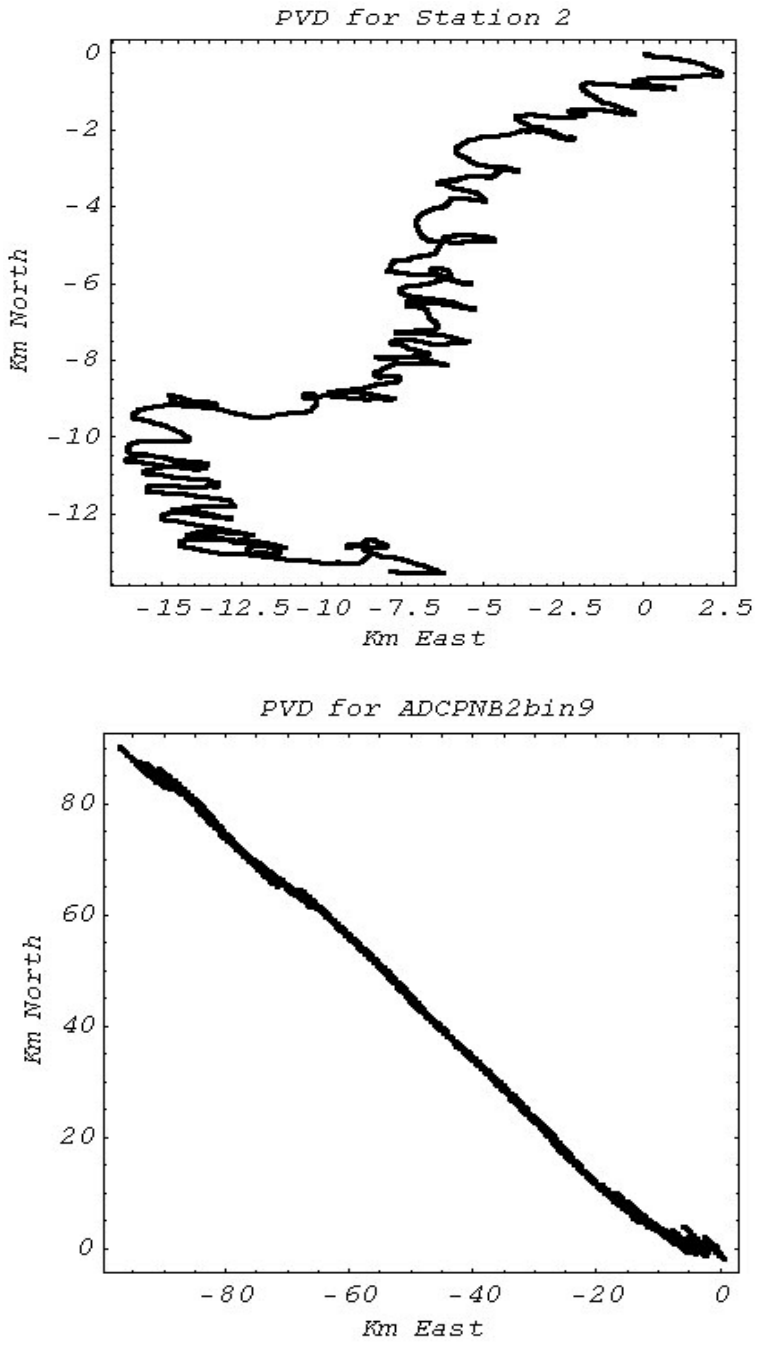

Figure 15. Progressive Vector Diagrams for (above) current meter N2 (near the National City Terminal) and (below) the ADCP (the Narrows, from a bin ~2 m below the MLLW). The net movement is to the SSW at N2 but to the NW at NB2. A progressive vector diagram represents the net transport that would occur, if the velocity field were spatially uniform and varied in time with the currents at the measurement location. In reality, a particle in the narrows will be transported either to a lower velocity environment in South Bay or seaward out of the estuary over a period of days to weeks. Note the differences in distance scales. Also, the ADCP record is ~65 days long, whereas the N2 record is only 19 d. Finally, the mean flow at N2 varies in direction over time, whereas mean direction is uniform in time at the Narrows.

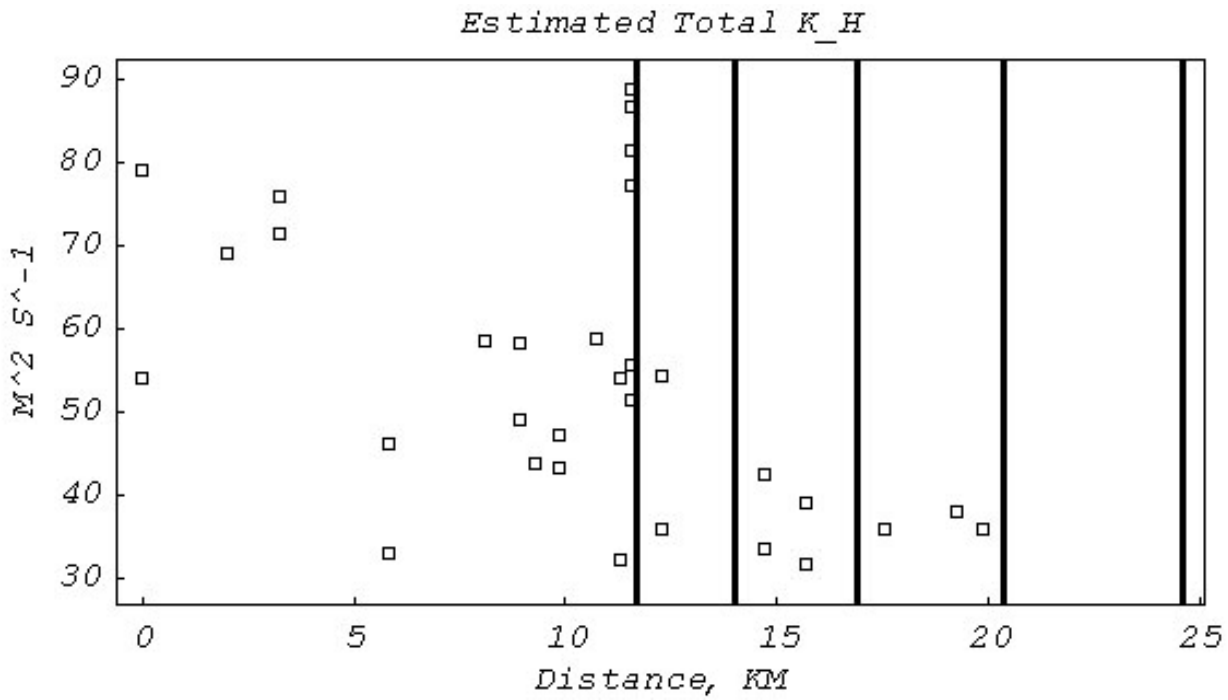

Figure 16. Spatial variations of the total tidal dispersion K_H estimated from current meter records located in the deeper channels. At and seaward of the Narrows, tidal pumping, an effect not readily estimated from the available current data is important, so the estimated K_H is likely somewhat low. As discussed in the text, the most landward three current meters in South Bay probably provide somewhat inflated estimates of K_H, because of their positions in locations where channel width changes abruptly. Still, the overall trend of K_H, small in South Bay, and increasing toward the ocean, with a local maximum at the Narrows is likely realistic. In effect, the Narrows is a physiographic boundary, because it functions as the mouth of South Bay. The vertical lines indicate the seaward boundaries of the four source volume sub-sections. Results for N5 are not shown here, because it is the only current meter not in a major channel.

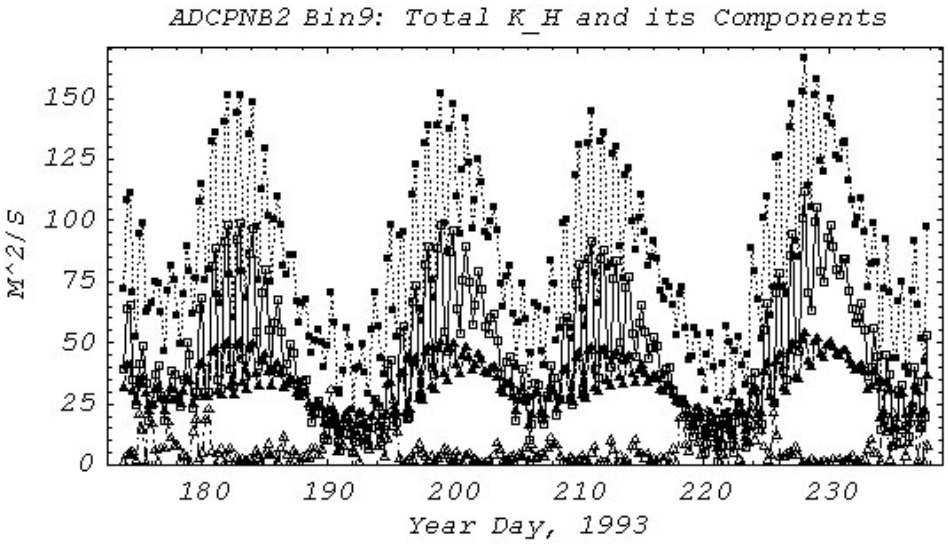

Figure 17a. A ~60 d calculation of near-surface longitudinal dispersion mechanisms for ADCP-NB2 (bin 9, at ~2m), showing estimated total longitudinal K_H (■), and its components K_{HL} (□), K_{HV} (▲) and K_{HR} (□). K_H is mostly due to lateral (K_{HL}) and vertical shear (K_{HV}). Streamline curvature (K_{HR}) is unimportant, and dispersion is strongest on spring tides. Tidal pumping (not estimated) may be important at this location. Note the substantial tidal daily variations.

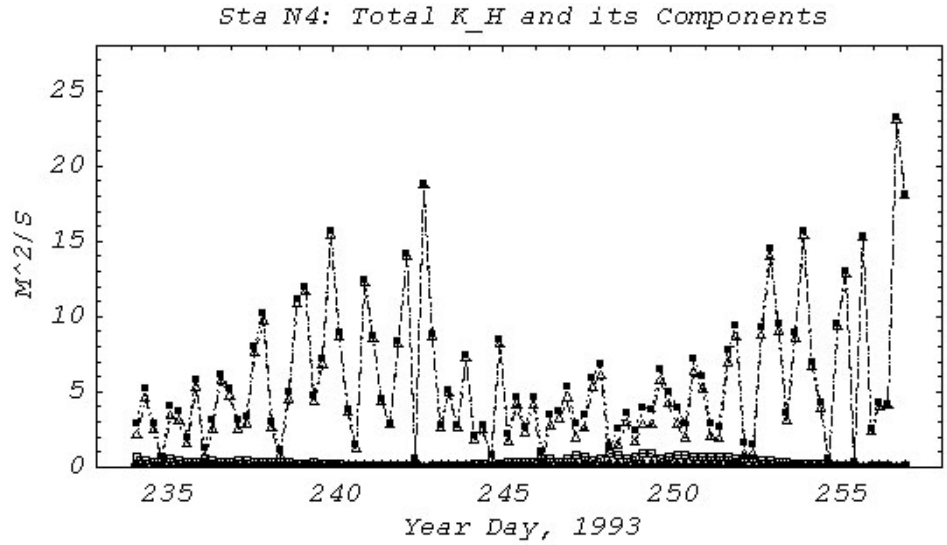

Figure 17b. A ~20 d calculation of near-surface longitudinal dispersion mechanisms at the N4 (in shallow water SE of Glorietta Bay); symbols as above. In this case, total longitudinal dispersion K_H is due almost entirely to tidal streamline curvature (K_{HR}); lateral (K_{HL}) and vertical shear (K_{HV}) are unimportant. K_H is largest on neap tides; tidal pumping is not likely to be important, because of the shallow depth. Results for this station are considered typical for most of South Bay. Tidal daily variations are occasionally strong.

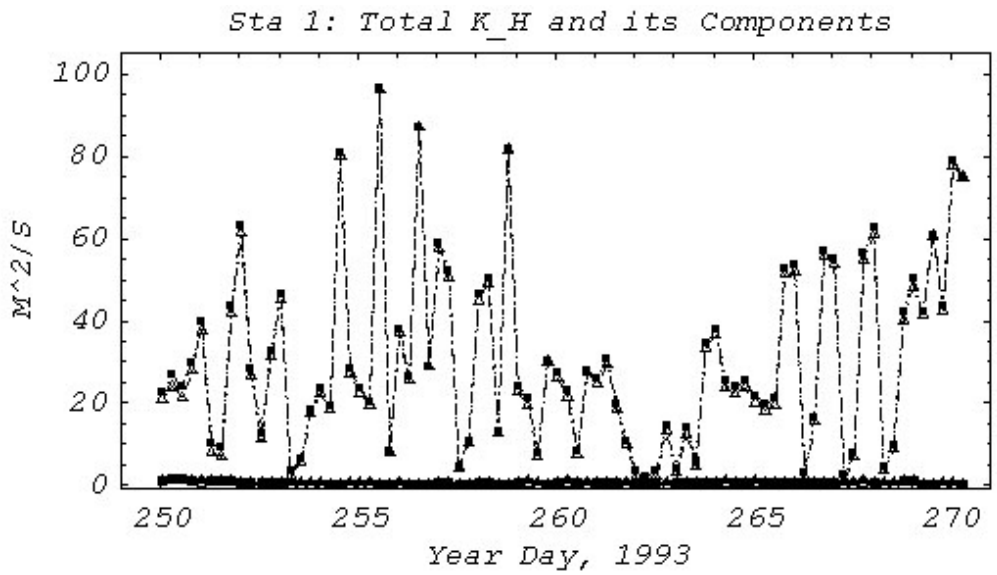

Figure 17c. A ~20 d calculation of near-surface longitudinal dispersion mechanisms at the N1 (near Sweetwater); symbols as above. As at N4, total longitudinal dispersion K_H is due almost entirely to tidal streamline curvature (K_{HR}); lateral (K_{HL}) and vertical shear (K_{HV}) are unimportant. K_H is largest on neap tides. Tidal pumping is not likely to be important, and tidal daily variations are occasionally strong. Results from Largier (1995) suggest that the spatially averaged dispersion in South Bay is not as large as estimated for this location.

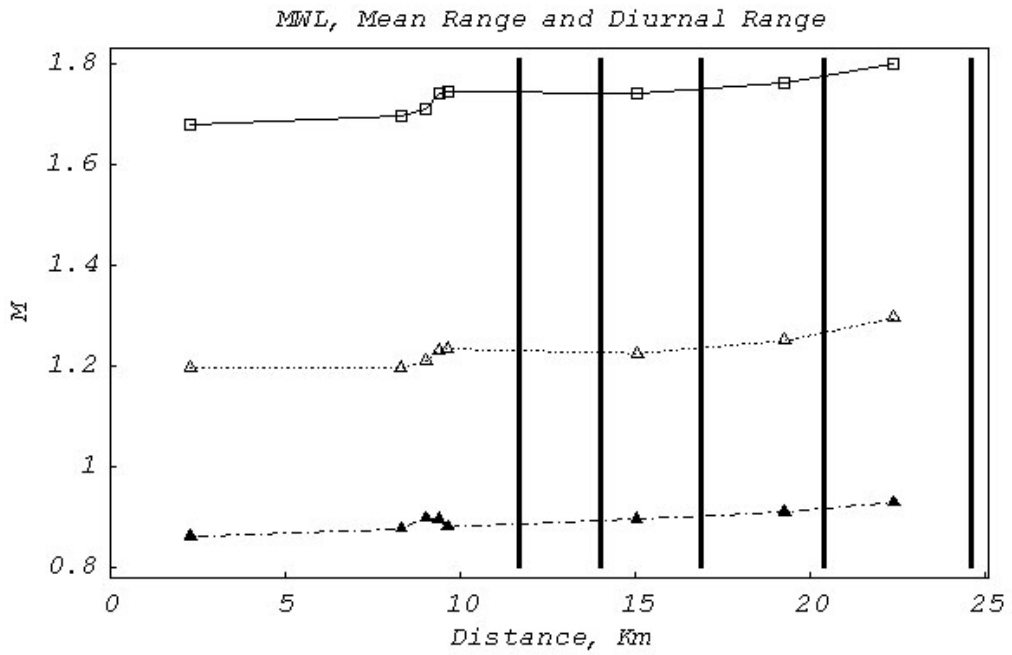

Figure 18. As a function of distance from the estuary mouth, Mean Water Level or MWL (▲) at bottom, mean range (□) (middle), and diurnal range ( ) (at top). Vertical lines indicate the boundaries of the four subregions of the source volume V_S.